

CTU Space
Research

Team 08 Technical Report to the 2023 EuRoC

Abstract

The Ilustria project's purpose is to move the CTU Space Research team forward to the higher category in rocketry. Our team has had so far experience only with rockets with an apogee of 1 km. With those rockets, we participated in our national competition Czech Rocket Challenge. The project's main focus is to involve as many students as possible in the development of an SRAD solution including the development of our own hybrid rocket engine. The rocket is therefore attending the EuRoC 2023 in the H3 category.

The Ilustria rocket is a modular rocket containing six sections connected to each other by aluminium RADAX joints. Sections alone are made of carbon fibre or glass fibre. The RadAx joints are the main component of a whole family of modular rockets which we are planning to develop in the future. The modular rockets represent a big potential for the next years of the EuRoC competition. We can easily interchange sections based on the rocket's purpose.

The payload for this year is a simple dummy mass of 1 kg with a shape of 100x100x100 mm, according to 1U CubeSat standard.

Contents

1	Introduction	4
1.1	Team Structure	4
1.2	Partners	4
1.3	Experience	5
1.4	Future	5
2	System Architecture	6
2.1	Overview	6
2.2	Propulsion Subsystem	7
2.2.1	Engine design	8
2.2.2	SRAD valves	8
2.2.3	Igniter	9
2.2.4	Fluid system	9
2.2.5	Nozzle dimensions	11
2.2.6	Grain geometries	12
2.3	Aerostructure Subsystem	14
2.3.1	Design And Calculations	14
2.3.2	Bearing Rocket Structure	17
2.3.3	RADAX Joints	17
2.3.4	Modules And Sections	18
2.4	Recovery Subsystem	22
2.4.1	Nosecone Ejection System	22
2.4.2	Parachute Design	23
2.4.3	Parachute Lines And Connectors	24
2.4.4	Initial Deployment Event	25
2.4.5	Main Deployment Event	25
2.4.6	Main Parachute Release Mechanism	25
2.5	Payload Subsystem	26
2.6	Avionics subsystem	26
2.6.1	Rocket Onboard Avionics	27
2.6.2	Ground Support Equipment	31
2.6.3	Flight Software	34
2.6.4	Ground communicator	38
2.6.5	Engine	38

2.6.6 Scheduler	38
2.7 Ground Station	38
2.7.1 Mission control application	39
2.7.2 HIL Simulator	39
2.8 Ground Support Equipment	40
3 Mission Concept of Operations Overview	42
3.1 Concept of Operations	42
3.2 Flight Performance	44
3.3 Trajectories and flight scenarios	45
3.3.1 Nominal flight	45
3.4 Flight events	45
3.4.1 Arming detection	45
3.4.2 Lift-off detection	46
3.4.3 Engine burnout detection	46
3.4.4 Apogee detection	46
3.4.5 Landing detection	46
3.5 Deployment events	46
4 Conclusions and Outlook	47
5 Appendices	49
5.1 System Data	49
5.2 Detailed Test Reports	51
5.3 Hazard Analysis Report	59
5.4 Risk Assessment	60
5.4.1 General	61
5.4.2 Propulsion	62
5.4.3 Structure	63
5.4.4 Recovery	64
5.4.5 Flight software	65
5.4.6 Electronics	66
5.5 Checklists	67
5.6 Engineering Drawings	77
5.7 Detailed Logical Process Diagrams	88

1 Introduction

CTU Space Research is a young student team founded in Spring 2021 at the Czech Technical University in Prague. Its purpose is to create and provide an environment for passionate students interested in aerospace engineering. They can improve their skills and put in practical use the knowledge they gain in lectures. Considering there is no Faculty of Aerospace Engineering at the CTU (only study programs) our team is a great opportunity for everyone who is interested in aerospace engineering and bring those people together.

1.1 Team Structure

Our team is divided into four basic engineering departments: Propulsion, Structures, Avionics and Payload. Those four departments are supplemented by two departments Management and PR. All of the departments have a Group Leader and a Deputy. In the case of Management, there is a Team Lead and a Team Lead Deputy. See table 1.1.

Department	Lead	Deputy
Avionics	Lukáš Mičan	Dominik Beňo
Payload	Danylo Zozulia	-
Propulsion	Daniel Hořejší	Bruno Heinich
Structures	Klára Čepová	Přemysl Čechura
Management	Viktor Hais	Michael Jurča
PR	Jakub Malínek	-

Table 1.1: Team Departments

1.2 Partners

Partners are divided into two main groups (based on their origin). Academical and Industrial. According to the amount of financial or material support, we divide the sponsor into four categories. See table 1.2

Our main partner is the Faculty of Mechanical Engineering which provides us with financial support and facilities such as an office or a temporary workshop. Other partners provide us with material or equipment for easier development of our rocket.

Amount [CZK]	Category
< 50 000	Partner
≥ 50 000	Bronze
≥ 100 000	Silver
≥ 250 000	Gold
≥ 500 000	Premium

Table 1.2: Partners categories

1.3 Experience

Our team has gained most of its experience participating in our local Czech competition Czech Rocket Challenge (CRC). Our team has participated in CRC every year since its foundation in 2021. The competition is helpful for team building and testing some of the essential systems, and procedures and to get the feeling of the competition spirit. Single members have gained a lot of experience from smaller projects in the past. For example development, testing and validating of a small hybrid rocket engine or developing a recovery system for atmospheric experiment. The team is very excited to gain even more experience at the EuRoC competition which we are planning to participate in every year to develop more skills for current and future students.

1.4 Future

The team's vision for the future is to build a stable background for university students including a permanent workshop and a professional rocket motor test facility. In the future, we want to start developing a liquid rocket engine and continue making improvements to our current hybrid engine.

2 System Architecture

2.1 Overview

The Illustria rocket is a 3520 mm tall modular rocket consisting of 6 sections (modules) with the outer diameter of 161 mm. It is powered by a SRAD hybrid engine. The connection between individual sections is provided by RADAX joints. By this technical solution we ensure good assemble ability and design variability for future projects. Each rocket section is equipped with module management board (MMB, codename "Zora"). Zora is a universal control unit to control peripherals of each module and power various electrical systems. Zora boards are interconnected with the flight computer by CAN bus.

Materials mainly used for the Aerostructure of Illustria rocket are carbon fibre composites (CFRP), glass fibre composites (GFRP) and aluminium 7075 T6. CFRP parts were mostly manufactured by the team's partner Compotech (composite technology and engineering company) using the winding technology (outer shell tubes). The engine cover with fins and the nosecone are manufactured by students using contact lamination into molds . GFRP was mainly used for prototyping. Due to the lack of radio wave transmittance through CFRP, the avionics module is the only module made from a GFRP wounded tube.

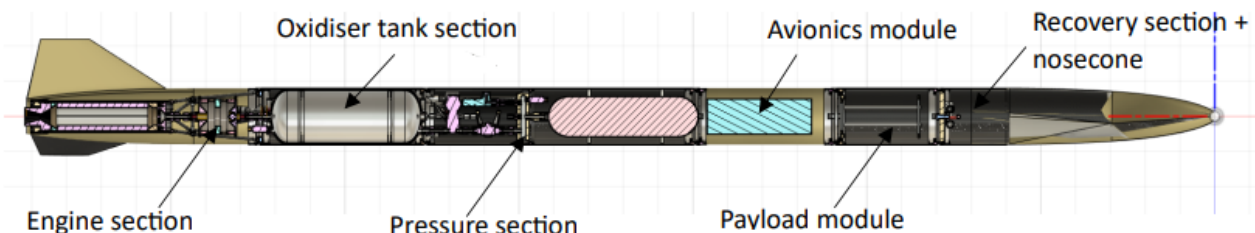


Figure 2.1: Rocket Cross-section

Parameter	Value	Unit
Flight Category	H3	[-]
Propulsion type	SRAD Hybrid	[-]
Length	3520	[mm]
Diameter	161	[mm]
Total Launch Mass	28.817	[kg]
Number of fins	3	[-]
Stability off the rails	1.509	[cal]
Launch rail exit velocity	30.458	[m · s ⁻¹]
Predicted apogee	3221.792	[m]
Predicted max acceleration	80.075	[m · s ⁻²]
Predicted max velocity	258.701	[m · s ⁻¹]
Predicted Flight Time	208.128	[s]

Table 2.1: General Specifications

2.2 Propulsion Subsystem

This chapter describes how the propulsion sub-team developed the hybrid rocket engine and how it will be operated in order to lift the Illustria rocket to an apogee of 3 000 meters.

Our hybrid motor is using nitrous oxide as the oxidizer and ABS as the fuel. It can reach a peak thrust of 1 800 N and provide a total impulse of about 9040 Ns.

The oxidizer tank of Illustria is structural part as well and thus developed by the structure sub-team. It won't be detailed here, in the propulsion documentation.

Parameter	Value	Unit
Total Impulse	9035.37	[N · s]
Maximum Thrust	1849.36	[N]
Average Thrust	1079.49	[N]
Burn Time	8.37	[s]
Launch Mass	3.7	[kg]
Dry Mass	2.4	[kg]
Fuel	ABS	[-]
Oxidiser	N ₂ O	[-]
Pressuriser	N ₂	[-]

Table 2.2: Engine Specifications

2.2.1 Engine design

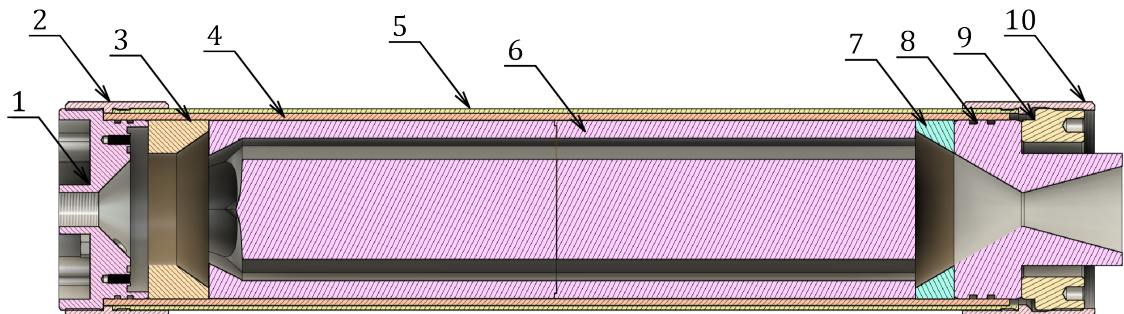


Figure 2.2: Motor

1 - Injector head (aluminium), 2 - Attachement for injector head (aluminium), 3- Top spacer/precombustion chamber (phenolic paper), 4 - Chamber isolation (phenolic paper), 5 - Engine case (aluminium), 6 - Fuel grain (ABS), 7 - Bottom spacer (phenolic paper), 8 - Nozzle (Phenolic paper), 9 - Hollow screw (aluminium), 10 - attachment for hollow screw (aluminium)

2.2.2 SRAD valves

For the control needs of the entire fluid system, a COTS ball valve motorization was developed for both the high and low pressure sections (see 2.3). 3D printed parts (yellow) made of HP PA12 nylon using MJF technology support the high torque servo on the valve body. The connection between the servo and valve axes is via an aluminum coupling. These servos have digital control and can operate the ball valves without problems.

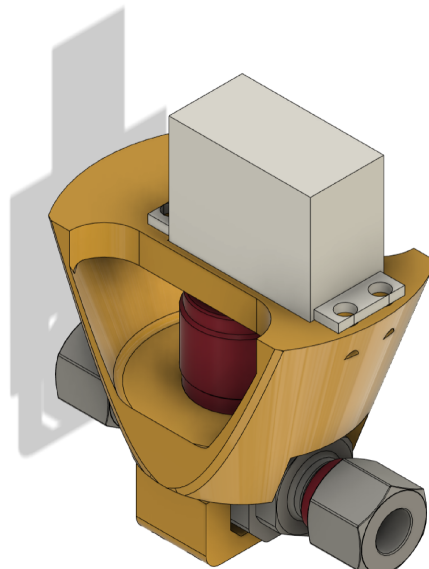


Figure 2.3: SRAD ball valve

The main engine valve is bi-stable electromagnetic valve, which was developed at University of West Bohemia by researchers for different project and thus is approached as COTS Valve.

2.2.3 Igniter

For igniter a mixture known as rocket candy was used. The mixture is composed of 65% potassium nitrate (KNO_3) and 35% sorbitol ($C_6H_{14}O_6$). Case for this mixture (2.4) is 3D printed out of ABS in a cone shape. The igniter (green) is lit by two electrical matches (red) for redundancy. These matches are commonly used for igniting small solid rocket motors.

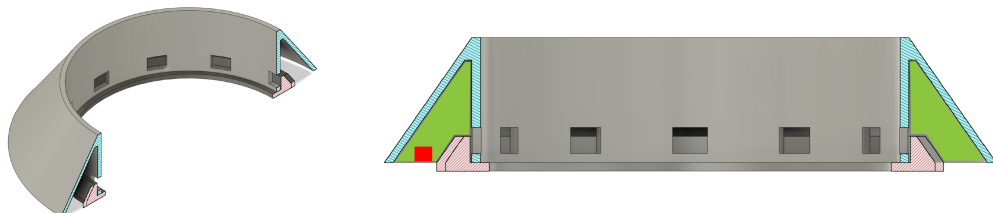


Figure 2.4: Back (left) and front views of igniter

When the engine is assembled, the E-matches are inserted into the ignitor, the ignitor inserted into the engine assembly, and the wires to the E-matches are routed through the nozzle out of the engine. During both HW and SW arming, when the rocket is on the launch rail, the wires to the E-matches are connected to the control cables. Arming is then done according to pre-launch procedure including HW and SW arming.

2.2.4 Fluid system

The entire power unit consists of three subsystems – the engine, the low pressure section and the high pressure section, see 2.5. The low-pressure section consists primarily of an SRAD tank containing an oxidizer with a nominal pressure of 50 bar. The tank design is discussed in more detail in the structural section of this report. The high-pressure section consists of a COTS pressurizer tank that helps maintain a constant flow of oxidizer to the combustion chamber. The high pressure section has a nominal pressure of 250 bar. Both sections are equipped with safety relief valves and pressure sensors in addition to the filling valves.

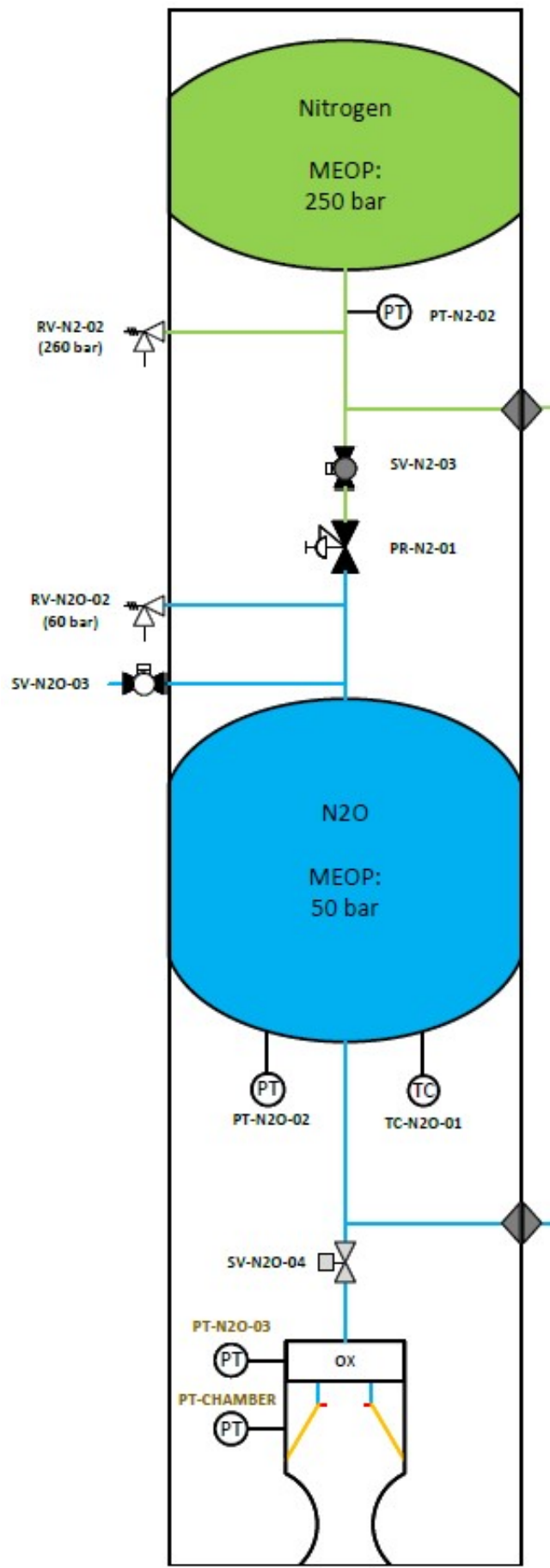


Figure 2.5: Fluid diagram

2.2.5 Nozzle dimensions

For the solid fuel of the engine acrylonitrile butadiene styrene (ABS) was chosen. This material is commonly used in additive 3D printing and so the grain can be produced easily in practically any desirable shape. It is also easily accessible due to its widespread use.

For oxidizer nitrous oxide (N_2O), also known as laughing gas, was chosen. It is widely used in the clinical practise as anesthetics and is increasingly popular in recreational use. This once again guarantees its accessibility. N_2O was to be used in liquid form at room temperature which necessitates storage pressures higher than 50 bar.

For the operation of the engine the following parameters were chosen:

1. Combustion chamber pressure $p_c = 3 \cdot 10^6 \text{ Pa}$
2. Thrust $F = 1800 \text{ N}$

For the characterization of the burn products and burn temperature data are available. For maximal specific impulse the targeted oxidizer to fuel ratio (O/F ratio) of 5:1 was chosen. This along with the chosen pressure determined the rest of the necessary characteristics of the products of combustion.

1. Chamber temperature $T_c = 3250 \text{ }^\circ\text{K}$
2. Specific heat ratio $k = 1.19$
3. Molar mass of combustion products $M = 0.0245 \text{ mol/kg}$
4. Prandtl number $Pr = 0.385$
5. dynamic viscosity $\mu = 9.4 \cdot 10^{-5} \text{ Pa}\cdot\text{s}$
6. heat of ablation $h_v = 2.42 \cdot 10^5 \text{ J/Kg}$

To calculate the important characteristics of the engine the following equations for isentropic flow were used. First the exit velocity v_e of gases from the nozzle was calculated:

$$v_e = \sqrt{\frac{2k}{k-1} RT_c \left[1 - \left(\frac{p_2}{p_1} \right)^{(k-1)/k} \right]}, \quad (2.1)$$

where p_2 represents the pressure at the nozzle exit. For maximum thrust this value should be equal to the outside ambient pressure p_3 . The engine was designed for sea level and thus the value of p_3 and consequently p_2 is equal to 101 300 Pa. R represents the universal gas constant and is equal to 8.314 J/mol·°K. For mass flow \dot{m} and the area of nozzle throat A_t the following expressions were used:

$$\dot{m} = \frac{F}{v_e} \quad (2.2)$$

$$A_t = \frac{\dot{m}\sqrt{kRT_c}}{p_1 k \sqrt{[2/(k+1)]^{(k+1)/(k-1)}}} \quad (2.3)$$

The value of nozzle throat radius r_t was than calculated using the A_t from equation (2.3). Than for the area of the nozzle exit A_e the following equations were used.

Where T_e is temperature of exiting gas and M_e is the Mach number at the nozzle exit. From this the value of exit radius r_e can be easily calculated. The nozzle exit angle was chosen to be 15° and the nozzle intake angle 35° . The resulting nozzle throat radius r_t and nozzle exit radius r_e is:

$$\begin{aligned} r_t &= 11.4 \text{ mm} \\ r_e &= 25.1 \text{ mm} \end{aligned}$$

2.2.6 Grain geometries

The regression of ABS was approximated using the following equation:

$$\dot{r} = \frac{0.635}{\rho_{fuel} P_r^{2/3}} \left(\frac{c_p(T_c - T_{fuel})}{h_\nu} \right)^{0.23} \left(\frac{\dot{m}_{ox}}{A_c} \right)^{4/5} \left(\frac{\mu}{h} \right)^{1/5}, \quad (2.4)$$

where ρ_{fuel} and T_{fuel} refer to the density and temperature respectively before ignition of the fuel. The expression was primarily derived to approximate the regression rate of fuel in grain with tubular core. However this geometry causes the O/F ratio to fluctuate greatly for a fixed oxidizer flow and would require unfeasible grain (approximately 1m for reasonable core diameter). In order to for the design to be feasible it was decided that a multi-core geometry would be used. However, several tubular cores positioned next to each other would pose a risk of a portion of the fuel separating from the rest and falling into the throat. This would most likely destroy the engine and also pose a large safety risk. Therefore different geometries were considered but equation (2.4) was still used to approximate the regression rate of the fuel.

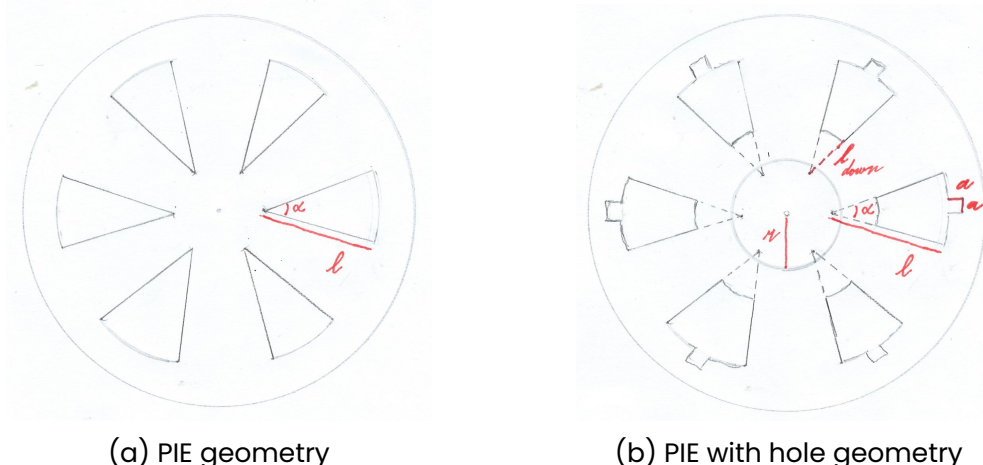


Figure 2.6

2.2.6.1 PIE geometry

The final geometry was created from a base geometry with alteration made afterwards while keeping the cross-sectional area of the core and the burn surface constant (two vital parameters that ensure correct fuel mass flow). The base geometry that was used can be seen in picture 2.6a.

2.2.6.2 PIE with a hole

However for $n > 6$ the distance between the tips of triangles was smaller than distance to the center of the grain, once again posing a risk of plugging the nozzle throat. Therefore an alteration to the geometry was made as can be seen in figure 2.6b .

2.2.6.3 PIE with a hole and hidden channels

Due to the evolution of the geometry during the burn itself the regression rate and consequently the amount of fuel released into the mixture is changing. Based on the equation (2.4) the O/F ratio increases as he burn progresses. As a result it would be beneficial if additional burning area was introduced during the burn. This is the purpose of hidden channels that can be seen in figure 2.7 (added channels compared to figure 2.6b). These channels are closed off from the injector and therefore do not burn from the beginning but only after the wall between them and opened cutouts burned through. The channels are open at the nozzle end to allow for balancing pressure within the channels and prevent a premature collapse of walls between burning and hidden channels due to high pressure. The dimensions of hidden channels are calculated to decrease the O/F ratio using the equation (2.4).

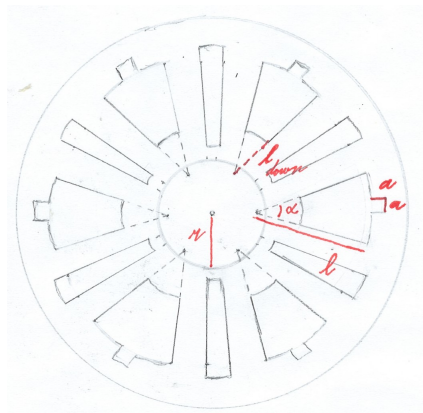


Figure 2.7: PIE with hole and hidden channels geometry

2.3 Aerostructure Subsystem

2.3.1 Design And Calculations

2.3.1.1 Expected Rocket Load

Since our team is without flight experience with this size of rockets, we have dimensioned the rocket's aerostructure based on the estimated loads for the entire life cycle, i.e., ground handling, launch and landing maneuver, and actual landing on the ground. According to the force analysis, we selected the following situations where the highest loads occur. The table below shows each situation, the type of loading, and the estimated load in terms of acceleration G.

Situation	Type Of Load	Acceleration [G]
Launch	Tension	4
1. Deployment Event	Tension	5
2. Deployment event	Tension	12
Landing	Compression	100
Side Fall	Bending	22
Manipulation	Bending	2
Flight Bending	Bending	Negligible Compared To Others

Table 2.3: Table Of Loads

For the calculation model, the rocket was considered as a rod with the distribution of mass points in the centres of mass of each section. The sections, their masses and dimensions estimates are shown in the table, the actual masses and dimensions have since been refined.

Sequence Number -	Section -	Mass [Kg]	Length [mm]	Position (from - to) [mm]
Origin				0
1	Nosecone	600	600	0 - 600
1	Recovery Section	2,64	185	600 - 785
2	Payload Module	3,24	300	785 - 1085
3	Avionics Module	3,64	400	1085 - 1485
4	Pressure Section	4,64	775	1485 - 2260
5	Oxidiser Tank Section	6,75	700	2260 - 2960
6	Engine Section	3,64	325	2960 - 3285
7	Engine	1,5	400	3285 - 3685
Total		29,35		3685

Table 2.4: Section data estimates for load calculations

The highest load in the rocket life cycle is the tension load when the main parachute is deployed, the impact on the ground stresses the structure in compression and the

subsequent fall to the side causes bending load. Bending load caused by handling was also evaluated. The loads on the individual parts can be seen in the following graphs.

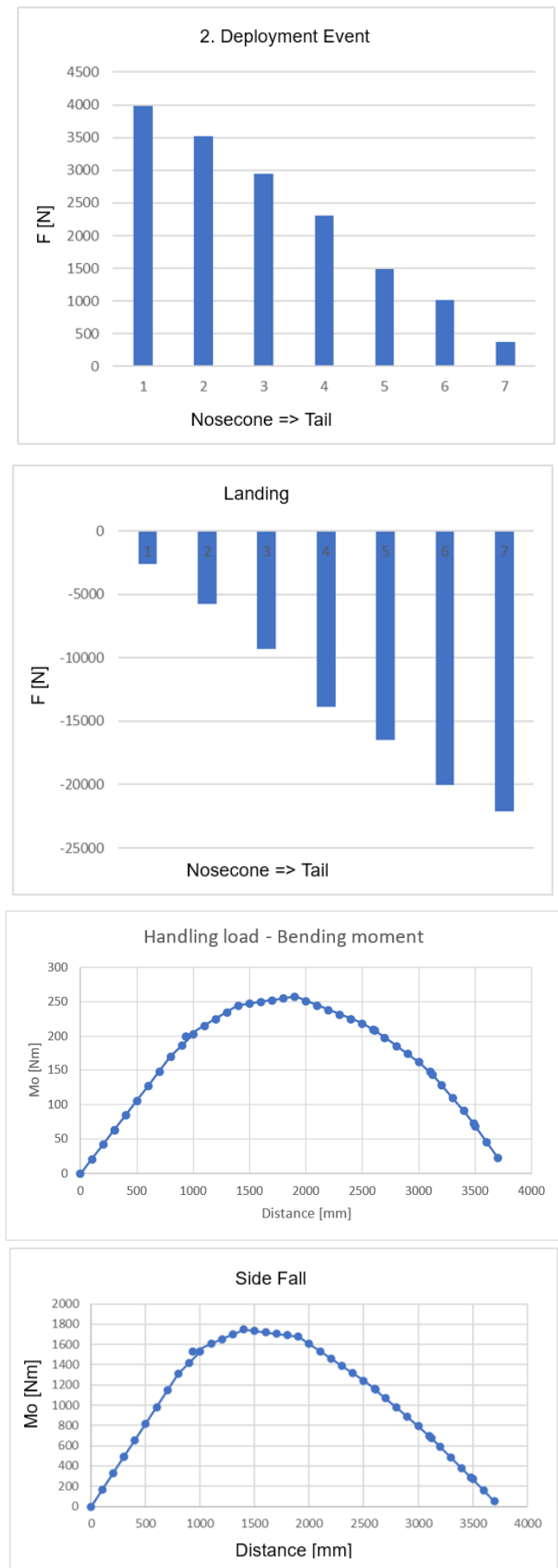


Figure 2.8: Important operational loads on the rocket structure

2.3.2 Bearing Rocket Structure

The main flow of forces throughout the rocket at all types of loads will be between the bulkhead mounted in the recovery section and the engine body. For the approach we have chosen, using a composite tube, the most mass advantageous transfer of forces is along the rocket's surface, i.e. through the hull composite tube. Due to the need for access to the engine, and a part of the pressure section, these sections are designed with the support structure inside the rocket and the actual hull tube acts only as an aerodynamic shroud.

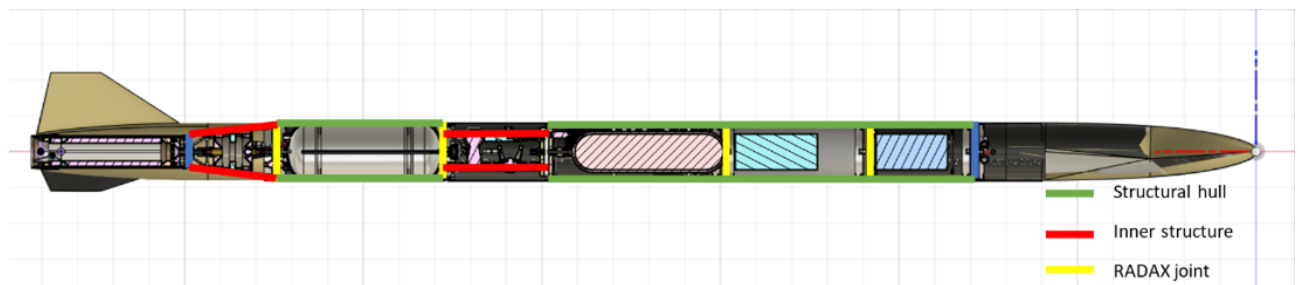


Figure 2.9: Forces Distribution Scheme

2.3.3 RADAX Joints

To create a modular rocket, a robust joint design had to be selected to connect the individual sections together. The RADAX joint was deemed to have the highest performance out of available designs. Our RADAX joints are based on the original RADAX concept and as such they employ two contact surfaces, one radial and one axial, which provide higher structural strength as opposed to a single conical contact surface.

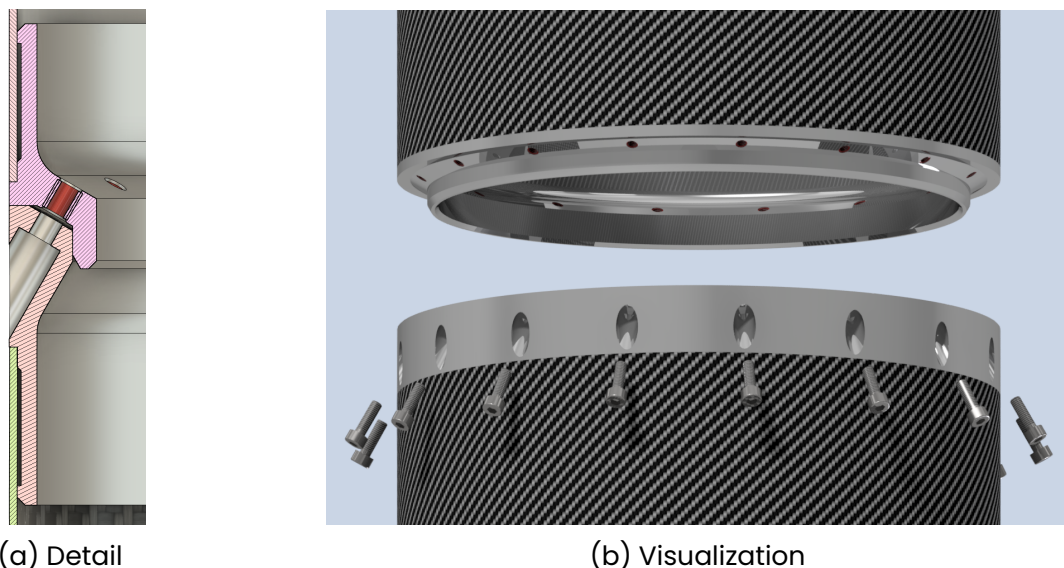


Figure 2.10: RADAX joint

The flanges of the RADAX joints are made of aluminium alloy EN AW-7075 T6. The bolted connection was designed and verified according to the ECSS-E-HB-32-23A Threaded

fasteners handbook. NASTRAN finite element method was used for parts of the analysis. After multiple iterations the design converged on using 16 high strength M3 bolts and Helicoil screwlock inserts for locking and thread reinforcement. The fastening torque was chosen as 1.8 Nm. Relevant margins of safety (MoS) according to ECSS are shown in the table below.

Failure mode		MoS	Value
Combined stresses in fastener during tightening	yield	$MoS_{ti,y}$	0,325
	ultimate	$MoS_{ti,ult}$	0,427
Axial stress in fastener due to preload and external load	yield	$MoS_{tot,y}$	0,556
	ultimate	$MoS_{tot,ult}$	0,717
Shear pull-out of thread		$MoS_{th,A}$	0,693
Crushing of flanges	yield	$MoS_{crush,y}$	0,863
	ultimate	$MoS_{crush,ult}$	0,353

Table 2.5: Margins of Safety according to ECSS during handling

While the RADAX joint geometry is the same across all joints on the rocket to ensure compatibility, various modifications were made to individual flanges to connect with other parts of the rocket, such as the motor mount, avionics bay, or parachutes. The RADAX flanges are connected to the structural composite hull using a glued joint.

2.3.4 Modules And Sections

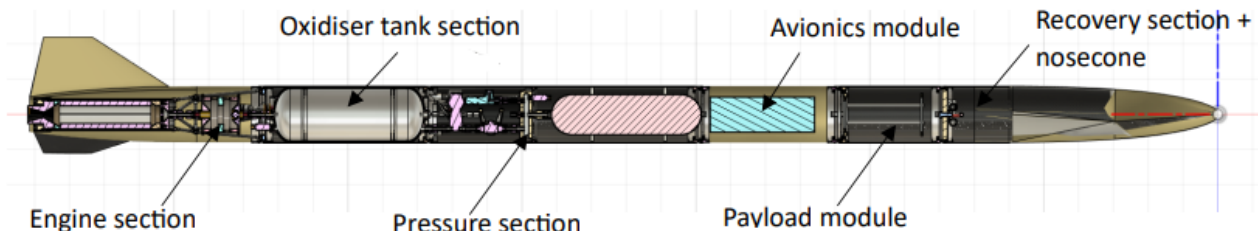


Figure 2.11: Rocket Scheme

2.3.4.1 Engine Section

The engine section houses the engine and relevant equipment, such as the main valve, oxidizer filling port and pressure sensors for the combustion chamber and injector. It also contains the nozzle extension. The structure of this section is composed of two structurally separate assemblies. The first one is the engine itself with its engine mount, which connects directly to the oxidizer tank section. The engine mount consists of a truss structure using woven CFRP tubes as beams, with nodes 3D printed out of metal. It can be split in half to allow easy access to the engine plumbing.

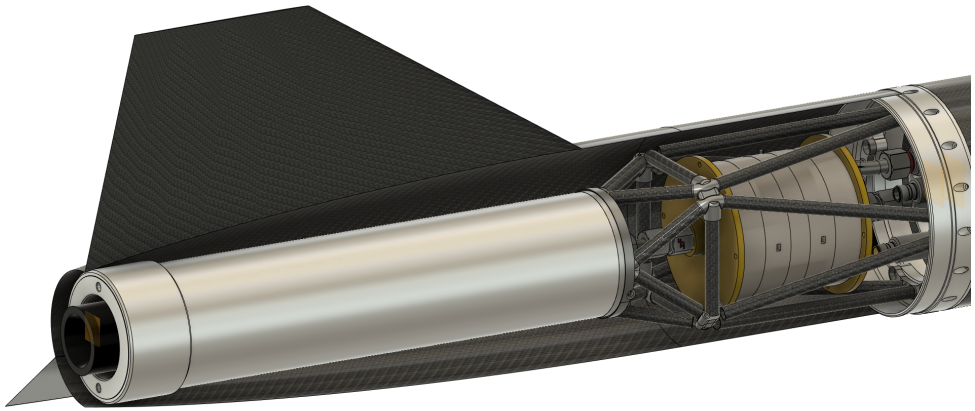


Figure 2.12: Engine section cutaway

The other part of the structure of the engine section is the CFRP engine cowling with integrated fins. It slides over the engine and connects to the oxidizer tank section with a RADAX joint. It does not transfer the thrust of the engine, but rather the bending loads associated with the aerodynamic fins. To ensure alignment of the fins, the whole part is laminated together using a special three part mold.

2.3.4.2 Oxidiser Tank Section

The Oxidizer tank is an integral part of the structure of the rocket and it is designed to withstand the relevant flight loads, but they are negligible when compared to the load imposed by the internal pressure in the tank. The tank consists of two semi-elliptical aluminium caps and an aluminium liner. All of these parts are overwrapped by a CFRP tube, which is the primary structural element of the tank. The liner was included to prevent contact between liquid nitrous oxide and CFRP. Highly chemically resistant FEP coated O-rings are used to create a seal between the liner and caps.

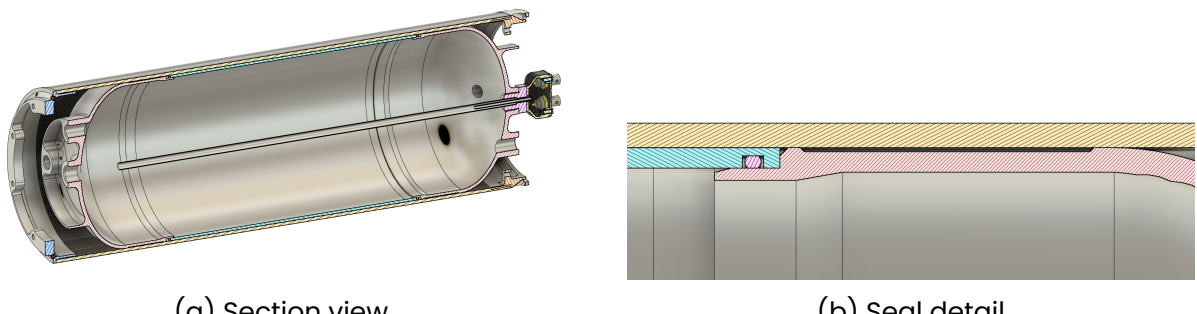


Figure 2.13: Main Oxidizer Tank

The oxidizer tank was designed to a burst pressure of 18 MPa, 3 times the maximum operating pressure of 6 MPa. There are 4 openings in each cap, which allow connecting propellant and pressure lines as well as various sensors (pressure, temperature and fluid level)

2.3.4.3 Pressure Section

The main purpose of this section is to provide and control pressure in the main tank. This section can be divided into two structurally different parts connected with a special coupling called K-connector (Aluminium 7075 T6) designed to reinforce the structure and provide support to the pressure systems -pressure tank, fittings, and valves. The pressure section is located between the avionics module and the oxidiser tank section. The upper pressure section consists of a pressure tank inside an inaccessible CFRP tube topped with a RADAX female joint providing connection to the Avionics module. The CFRP tube is glued to both the K-connector and the RADAX female joint.

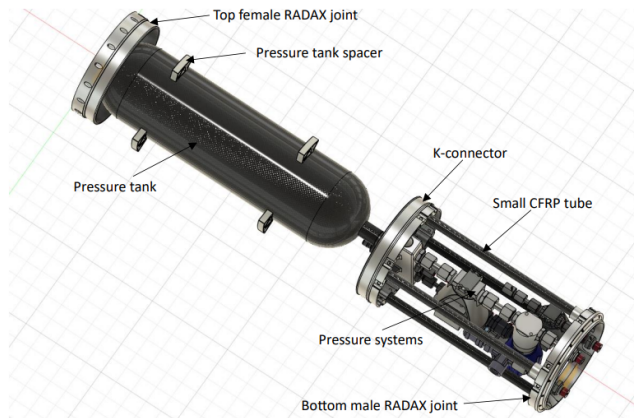


Figure 2.14: Pressure Section Scheme

The lower part is fully accessible, four small CFRP tubes provide necessary support, while the outside shell (CFRP tube vertically split in half), which is held in place by screws, can be removed. This solution allows access to crucial parts of the pressure system. Small CFRP tubes are glued into the K-connector from top and into the altered male RADAX joint from the bottom.

2.3.4.4 Avionics Module

The purpose of this module is to protect the flight computers and allow the rocket to communicate with the base. In addition to the flight computers, there is also a wireless charger in this section. The hull is a GFRP tube with an access hatch. The computers are housed in a special 3D printed case, the case is screwed to the female RADAX joint on top of the module.

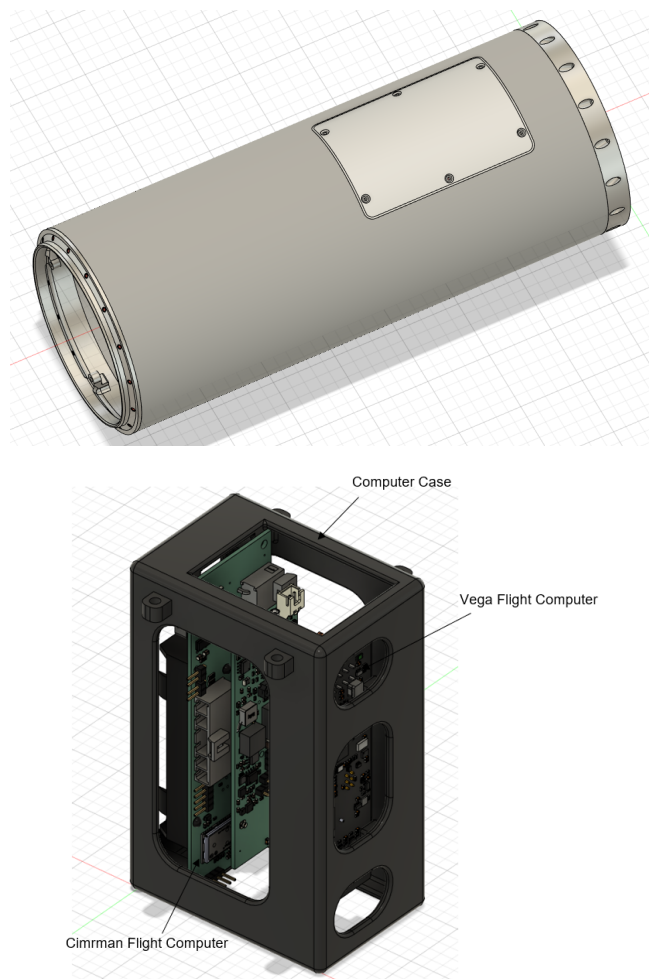


Figure 2.15: Avionics Section

2.3.4.5 Payload Module

Payload module is located between the recovery section and the avionics module. The section is connected with RADAX joints on both sides – male RADAX joint on the bottom, and female RADAX joint on the top. The purpose of this section is to hold the payload in place with a custom structure. This structure consists of two Nylon PA12 holders and CFRP tubes and is screwed to the male RADAX joint on the bottom. The connection between the CFRP tubes and the printed parts is ensured by a glued joint.

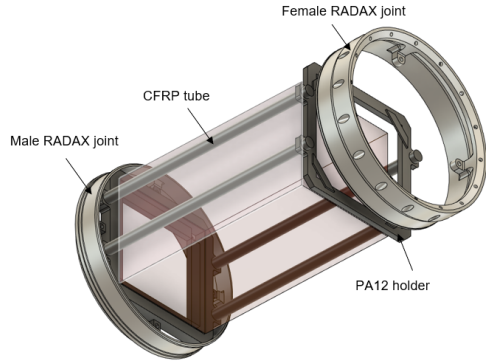


Figure 2.16: Payload Section Scheme

2.3.4.6 Recovery section And Nosecone

The recovery section is located on top of the Illustria rocket. The main purpose of this section is to house the SRAD recovery system. A CFRP tube acts as a hull. The CFRP nose cone is partially inserted into the hull and secured with shear pins. Ballast is included in the nose cone to improve the stability of the rocket. Both Pyro Valves are mounted on the recovery RADAX, with an eye bolt in between them. The eye bolt holds the parachute lines and is the only connection between the rocket and the parachutes. The recovery RADAX has a single sealed passageway for all the necessary avionics connections.

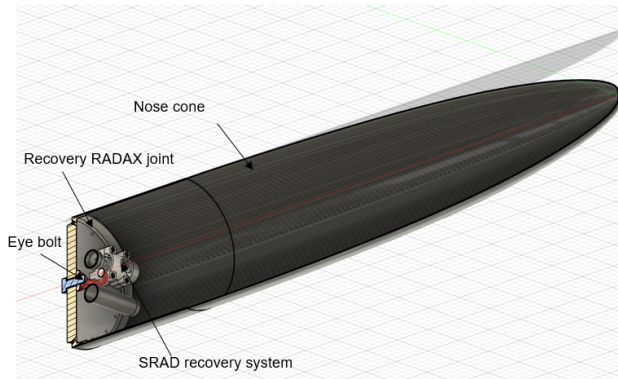


Figure 2.17: Recovery Section Scheme

2.4 Recovery Subsystem

2.4.1 Nosecone Ejection System

The initial deployment event is executed by a pair of SRAD ejection systems. The “Pyro Valve” works by piercing a 20g CO₂ cartridge by propelling a piston with a spike using a black powder charge. The CO₂ pressure breaks shear pins around the interface between the nosecone and the airframe and deploys the nosecone.

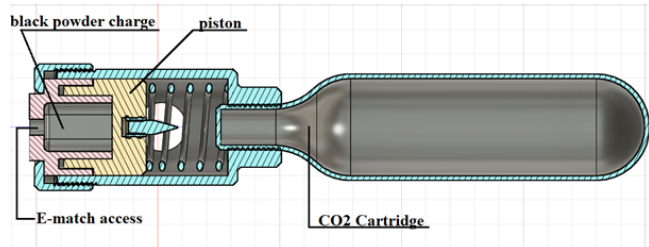


Figure 2.18: Internal Pyro Valve Layout

Each Pyro Valve is equipped with 2 igniters, each operated by a different recovery avionics system. In standard atmospheric conditions each 20g cartridge represents 10,75 litres of volume.

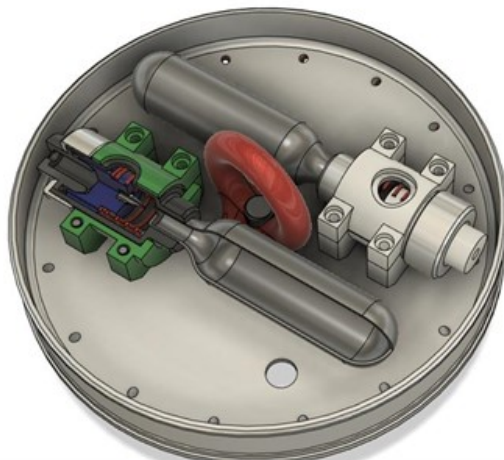


Figure 2.19: Packaging Layout On Recovery RADAX

2.4.2 Parachute Design

The drogue and the main parachutes are designed to slow the descent of the rocket down to the final landing velocity of 7 m/s. The design and size of these parachutes were based on the estimated dry weight of the descending rocket - 23kg. Parachutes were manufactured by students. Thus, the number of gores was set to only 12 per parachute, since this number makes the manufacturing process easier. Consequently, each parachute has 12 lines. The shape of an opened parachute is semi – elliptical.

	Diameter [m]	Spill Hole Diameter [m]	Line Length [m]	Number Of Gores	Parachute slider diameter [m]	Colour
Drogue Chute	0,7	0,04	1,5	12	0,09	Bright green
Main Chute	2,8	0,14	5	12	0,27	Black

Table 2.6: Parachute Design

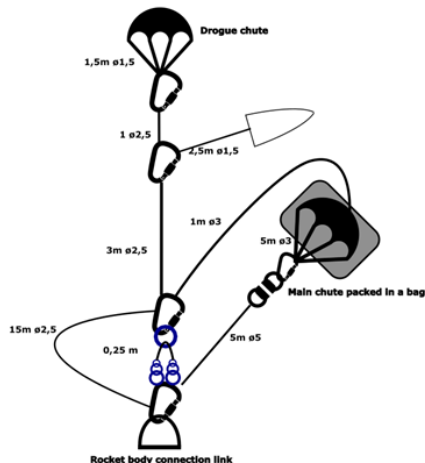
Each parachute also features a slider. The purpose of these sliders is to reduce the high momentary acceleration that occurs as a result of a rapid parachute opening. A slider ensures constant distance among individual parachute ropes. This, combined with the aerodynamic drag of a slider, creates forces that actively act against the opening of the parachute. The high G forces are significantly lowered, due to the slower opening of the parachutes.



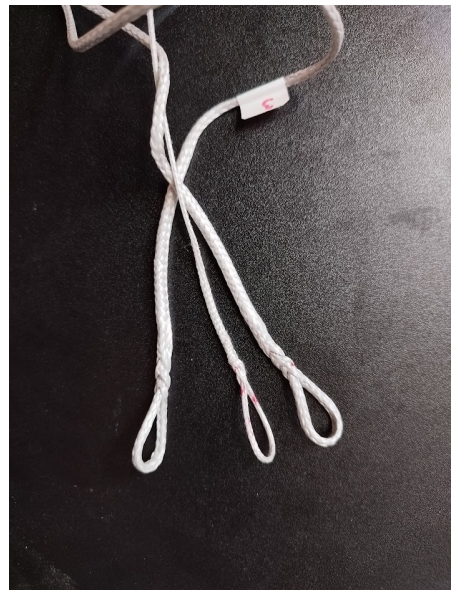
Figure 2.20: Drogue Chute Slider

2.4.3 Parachute Lines And Connectors

Lines of each parachute are connected to snap hooks. Additionally, a swivel link is connected to the main parachute snap hook. Parachute lines, as well as all the other connection lines, are Dyneema® ropes of marked lengths and diameters. Dyneema® ropes were chosen for this purpose because of the ability to make loops without the use of knots which negatively impact the performance of any rope. On the diagram below are displayed all line connections regarding the recovery system.



(a) Lines Diagram



(b) Line Loops

Figure 2.21: Parachute Lines And Connectors

2.4.4 Initial Deployment Event

The initial deployment event begins when the nosecone is ejected - 1 second after reaching the apogee. The ejection pulls out the drogue chute, links and main parachute folded in the containment bag out of the nosecone, allowing the drogue chute to inflate and slow the rocket down to 23 m/s.

2.4.5 Main Deployment Event

The main deployment event begins when the rocket reaches the altitude of 450 m AGL. The purpose of this procedure is to deploy the main parachute to reduce the velocity of the rocket during descent even further, reaching the final velocity of 7 m/s. During this procedure the tense line between the drogue chute and the body of the rocket is eliminated, allowing the drogue chute to pull off the containment bag covering the main parachute. Once the bag is pulled off, the main parachute inflates, and the rocket continues to descend.

2.4.6 Main Parachute Release Mechanism

To eliminate the tense line of the drogue chute, a three-ring mechanism is implemented. It allows a loop of rope with diameter of 1mm to securely hold the mechanism intact, securing the drogue chute line together. When time comes to deploy the main parachute, a section of the loop is pyrotechnically burned off, which releases the three-ring mechanism and eliminates the tense drogue chute line. There are two exact copies of this mechanism implemented in parallel. Each of these copies is wired with two pyrotechnic igniters. Each igniter operating on a respective copy is controlled by one of two different

computers. Therefore, one computer can single-handedly set off the igniters on both copies, while a successful release of a single mechanism is enough to start the main event.



Figure 2.22: Three-ring Mechanism

2.5 Payload Subsystem

The payload is dummy mass of 1kg in shape of standart 1U CubeSat (100x100x100 mm).

2.6 Avionics subsystem

The avionics subsystem is composed of 3 main parts: onboard avionics, ground support equipment (GSE) and ground station. These parts cooperate to provide all required features. The rocket onboard avionics manages everything related to the rocket and its flight, such as valve actuation during engine start or recovery system actuation during flight. The ground support equipment provides functions to safely load and unload oxidizer from the rocket as well as the ability to measure data from sensors during engine tests. The ground station can operate both the ground support equipment and rocket onboard avionics to allow safe control of oxidizer loading and rocket ignition and to help with rocket recovery after landing.

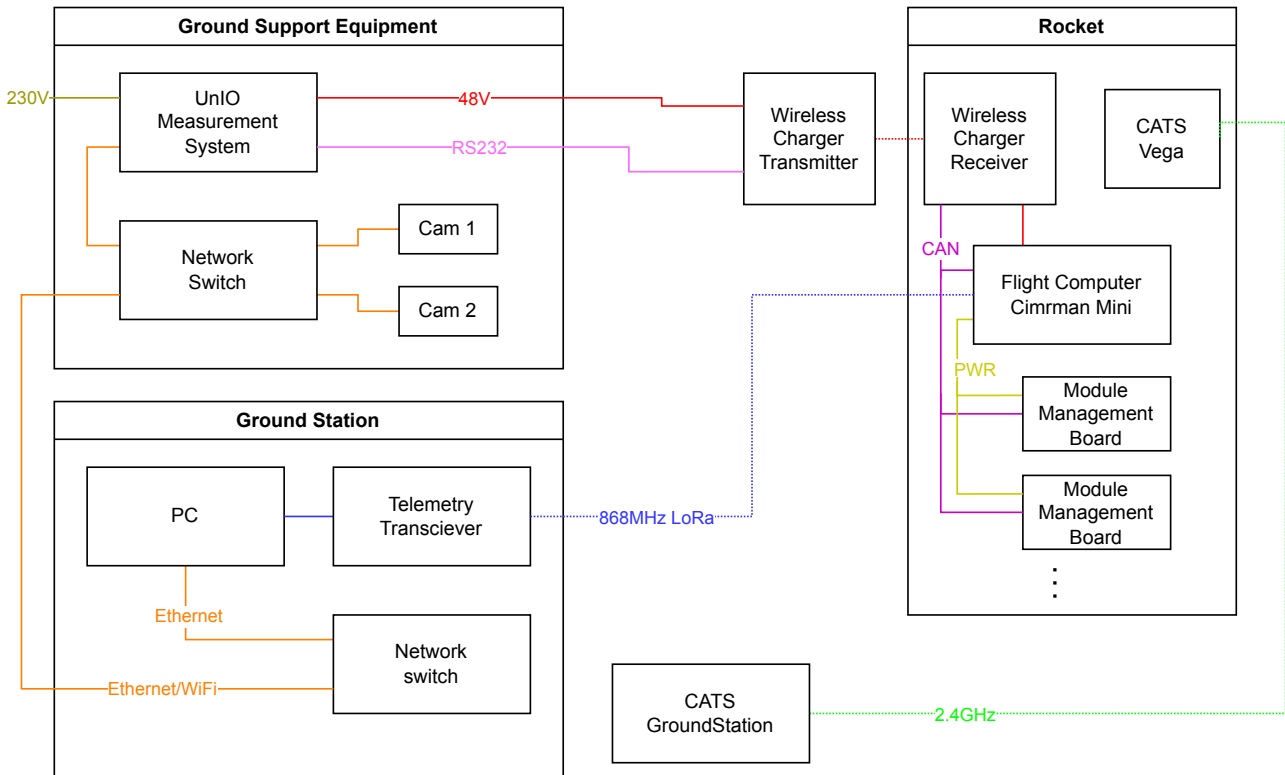


Figure 2.23: Complete avionics system architecture

2.6.1 Rocket Onboard Avionics

2.6.1.1 Architecture

Since the main concept of the whole rocket is modular, the architecture of rocket onboard avionics also follows this direction. It is composed of a main onboard flight computer unit Cimrman Mini with multiple Module Management Boards placed in different rocket modules. The flight computer acts as the “brain” of the rocket and the Module Management Boards control all actuators and digitize data from sensors. The flight computer and all Module Management Boards communicate through CAN bus that ensures reliable data transmission with minimal cabling required. Therefore, it is fairly simple to change the configuration of the rocket modules as needed. To ensure reliable connection, a locking Molex connectors are used along with cryo-compatible cabling.

The avionics parts are interconnected through a 6 lane Rocket Bus with 2 of the lanes used for CAN communication between the flight computer and the local control units, two lanes used for power distribution with voltage between 7 and 8,4 Volts and the last two lanes are intended for future use in the follow up projects. This architecture can be seen in the picture below.

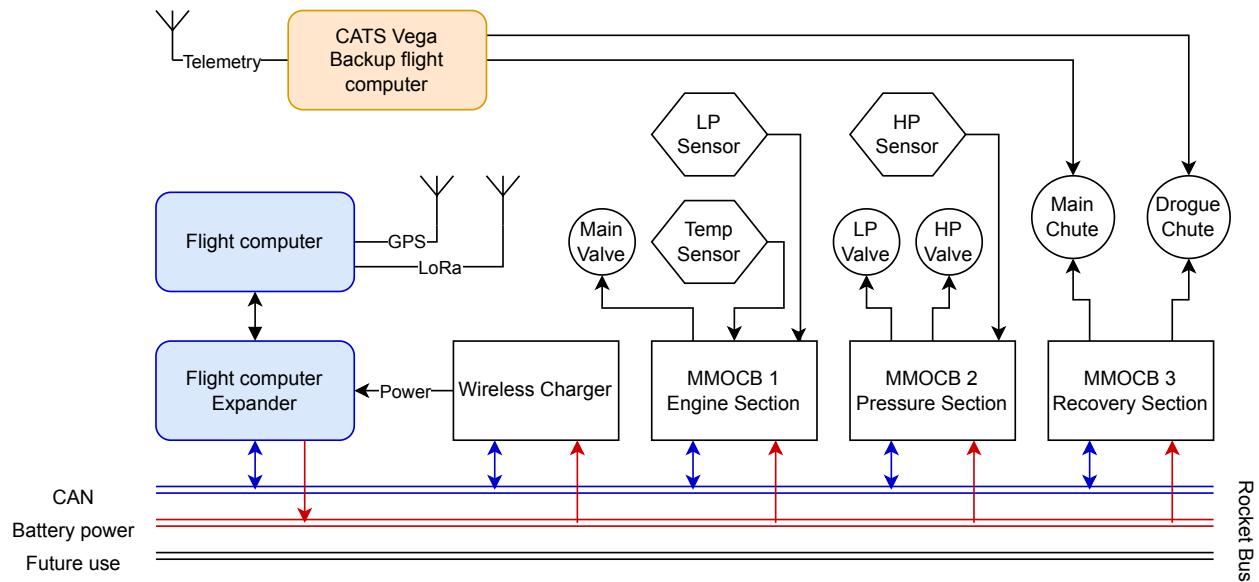


Figure 2.24: Onboard avionics architecture

When standing on launch pad a wireless charger is used to power the rocket and it also facilitates communication between the ground station and the rocket avionics. This ensures virtually unlimited time for standing on the launch pad because the batteries are not being discharged and in addition can be charged up if needed.

2.6.1.2 Primary Flight Computer

The heart of the computer is the STM32WLE5JC microcontroller in the LoRa-E5 module, which manages a set of sensors, inputs and outputs for controlling the entire rocket including the recovery system. The flight computer's design choices focus on maximum reliability and versatility. It was expected that the flight computer would operate in an environment with intense vibrations and accelerations and at the same time it should be flexible enough to accommodate various different mission requirements.

Cimrman Mini has already shown that versatility is indeed one of its strong points - with a clever usage of its outputs and pin headers, the flight computer was flown to approximately 34 km above sea level in a probe on a weather balloon, gathering data and heating up sensitive equipment and batteries. The outside conditions were truly harsh, with a recorded probe surface temperature of -22°C and surrounding air temperature down to -50°C . The whole flight lasted for more than two hours. Moreover, Cimrman Mini has already been flight tested on a rocket as well. Acting as the main flight computer for a CTU Space Research's experimental rocket in a Czech Rocket Challenge competition the flight computer performed nominally with correct detection of all flight phases even though the rocket experienced issues with the engine and thus didn't reach the target apogee. EUROC will be no exception to this versatility rule. The flight computer is augmented with an expander board that allows communication with all the other parts of avionics in the rocket.

Regarding the hardware, the flight computer is equipped with a basic set of

sensors necessary for detecting the rocket's launch and apogee - a barometric altimeter, accelerometer, and gyroscope. It also includes additional sensors such as a magnetometer and thermometer. Additionally, signals from the processor including SPI and I2C buses are exposed on pin headers, allowing for the connection of external components or modules. For data storage, the computer is equipped with 4 megabits of EEPROM memory. To aid in locating the rocket after landing in tall grass, it also includes a 100dB buzzer. For communication with the computer for firmware configuration or downloading measured data, an FTDI serial-to-USB converter is used, and a USB C connector is mounted on the board. The main source of energy is the battery. The flight computer is very flexible in terms of power - it can use input voltages from 3.8-16V, which corresponds to LiPo batteries with one to four cells. For backup power, a supercapacitor is used, capable of keeping the flight computer operational for at least 60 minutes without a main battery power source. Cimrman Mini also includes a power output, which is controlled by a low-side MOSFET.

The LoRa-E5 MCU used in this setup also includes RF circuits for possible wireless communication using LoRa modulation. The RF trace from the microcontroller can lead to a U.FL connector or, through a balun, to two symmetrical pads on the edges of the board. This allows for various antenna options as needed.

Regarding the expander board, it adds functionality to the Cimrman Mini needed for controlling a rocket of this size. The board provides a bridge between SPI in Cimrman Mini and CAN bus, which is used for communication throughout the rocket. The expander also acts as a power supply for the whole rocket. It handles charging of two Li-Ion batteries from wireless charger power input and supplies the power to the rest of avionics. In addition, the flight computer is capable of measuring the power draw. Another important addition is GPS receiver which is not present on the bare Cimrman Mini flight computer. The expander also accommodates multiple connectors for reliable connection to other avionics parts.

2.6.1.3 Module Management Board

The module management board (MMB, codename "Zora") is a universal control unit subordinate to the onboard flight computer of the rocket. Its main task is to control all actuators and sensors in the rocket module and to act according to instructions given by main flight computer, as well as providing power to the various electrical systems stored in these modules. As described in previous paragraphs, the Module Management Board is connected to the rest of the avionics through a Rocket Bus that supplies power and CAN bus communication.

The Module management unit itself has 3 basic parts. The MCU with added CAN Transceiver enabling communication via the CAN bus, the power management system consisting of two further subsystems and several peripheries. We will now dedicate our attention to these systems.

The power management system consists of the Supercapacitor subsystem, which is a failsafe system consisting of four supercapacitors and the hardware for their safe

charging. This system is designed to kick in case the battery power voltage falls unexpectedly or drops completely, to supply the whole section for the longest time possible after such event. It is also responsible for powering two H-Bridges as well as up to four general purpose input output connections with high current delivery capability. The power supply system then is responsible for supplying the rest of the board with 3,3 V, 5V and 12V. There are four LEDs indicating if all four voltage lanes are powered.

The MCU is connected directly to the CAN transceiver for communication with the flight computer as well as being connected to all the peripheries to enable the measurement of raw data which can then be transmitted to the flight computer for evaluation and then to the ground station. The MCU is connected to an SWD, Serial Wire Debug, port intended for programming and debugging of the board.

The board supports a plethora of peripheries, including two H-bridges, one integrated H-bridge and one high current H-bridge for opening and closing of valves or control over other igniter or motor driven systems. The board also includes four current loop inputs for connection of sensors, supporting 3,3 or 12 Volt power supply. Then there are four general purpose input output connections (GPIOs). Which can be powered either by 3,3 or 8 Volts, depending on the hardware connected. The list is finished by an I2C connection and two UART connections to enable easy future expansion. The systems and architecture described above, can be seen in a diagram below.

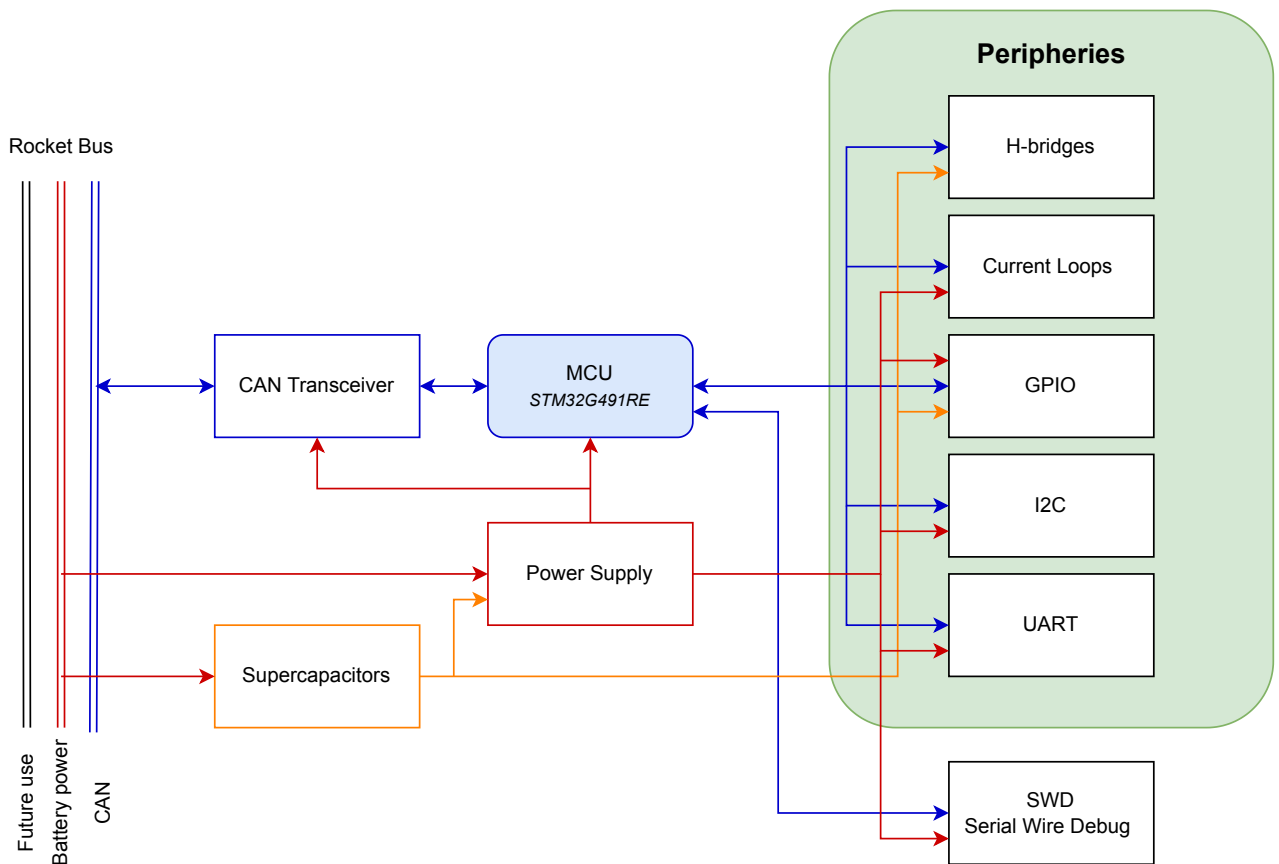


Figure 2.25: Module management board block diagram

2.6.1.4 Wireless Charger

The wireless charger system serves a dual purpose: it charges the rocket's battery pack and facilitates communication between the Primary Flight Computer and Ground Station. This system comprises two essential components: a transmitter and a receiver. The core function of the wireless charger is to maintain a constant voltage of 30 V DC on the receiver's output for the whole output power range from 1.5 to 35 W.

The architecture of the wireless charger is based on the Qi Standard which utilize inductive power transfer to transfer both power and data between the transmitter and the receiver.

The transmitter's core architecture features an H-bridge inverter composed of MOSFETs and gate drivers, a series resonant circuit incorporating a custom-wound planar coil using Litz wire and C0G ceramic capacitors. Similarly, the receiver's core architecture comprises an H-bridge rectifier with Schottky diodes, and a series resonant circuit equipped with a custom-wound planar coil and C0G ceramic capacitors. Both resonant circuits are tuned to the same frequency of 100 kHz.

We utilized a novel optimization method to calculate the parameters of the coils and input voltage. The input voltage at the transmitter's power input is 48 V DC. As a result of these optimizations, the wireless charger system achieves an impressive overall DC-DC efficiency of 81% when operating at the nominal charging power of 30 W.

2.6.2 Ground Support Equipment

2.6.2.1 Architecture

The ground support equipment is controlled with an SRAD modular Universal Input Output (UniIO) system. The main philosophy behind its design was to make it reliable and simple to set up in various scenarios. For that purpose, the system consists of different modules that connect to the motherboard with central microcontroller that runs main system services. The system design exposes many common buses (SPI, I2C, GPIO) and thus allows for design of various modules ranging from low-cost digital or analog input modules to high performance control modules with dedicated microcontroller.

The system physically consists of a motherboard into which modules for controlling and measuring different elements are plugged in. The motherboard and modules are placed into a chassis that can be mounted in a 3U slot on a standard 19inch server rack. The whole electrical side of GSE is then contained in a 4U strengthened box for easy transport. Additional networking or power delivery equipment can be transported alongside it as well.

The system is compatible with the SCPI protocol, making it compatible with many existing software measurement solutions. Connection with the computer is then achieved over Ethernet, USB or RS232 interface.

2.6.2.2 UnIO Motherboard

The motherboard is the backbone of the UnIO measurement system. It houses all communication with the outside world as well as acting as the brain for all attached modules. Up to eight modules can be plugged in at once. Each module is provided with 3.3V, 5V and 12V power supply rails alongside serial bus interfaces SPI and I2C and dedicated GPIO interfaces with interrupt capability. For connecting the modules, a PCIe 4x physical connector is used on the motherboard as that allows for a further decrease in module manufacturing costs.

2.6.2.3 UnIO Modules

There are currently six fully developed modules for the UnIO measurement system. Each module acts as a subordinate to the motherboard. For communication, all SPI and I2C links and GPIO interfaces are provided. Each module may choose to use either of these depending on its requirements.

Current Loop The current loop module is used for measurements with standard 4-20mA current output industrial sensors. It contains 16 independent channels. Digitization is achieved by measuring voltage drop on a shunt resistor in line with the current loop flow. The voltage is then sampled by a 12-bit ADC. The ADC communicates with the main measuring system via SPI. Averaging can be applied to increase the precision of measurement. Depending on the averaging setting, up to 200sps with all channels active can be achieved.

All channels have been calibrated using a HP 34401A multimeter. After calibration, the system achieves an average error of less than 0.01mA or less than 0.1% FS across all channels. Each current loop is equipped with a polyfuse for safety in case of bad connection or malfunction. The current loop module is equipped with round screwing connectors for connecting the sensors.

IOCard The IO module is used for controlling testing setups and GSE. It contains the following IO capabilities:

- 12 GPIO pins with configurable voltage levels
- 4 power outputs capable of driving up to 500 mA sustained or 1A in a pulse
- 4 analog inputs
- I2C interface with configurable voltage levels for expansion
- Serial servo interface
- 3 H-Bridge drivers capable of delivering up to 6A of power

All operations are orchestrated with a STM32L010 microprocessor. It communicates with the motherboard through SPI. There is also an on-board serial which can be used as

either an alternate source of control or for debugging. All digital inputs are protected against potential over voltages. For driving the high-power outputs and H bridges, external 12V or 5V input rails are provided for high current applications.

The IOCard is programmed with a set of actions it can perform. This eases the burden on the rest of the measuring system and allows for use in system control applications. Although having direct control over the module enables a lot of flexibility, in practice, we usually only ever want to perform a small set of actions such as “open fill valve” or “fire igniter”.

LoadCell The LoadCell Module is used for measuring tensometric load cells configured as a Wheatstone bridge. It allows for concurrent measurement of 4 channels, each with dedicated ADC and a voltage regulator. The ADC measures differential voltage across the Wheatstone bridge with programmable 64x or 128x gain and sample rate up to 80 samples per second. It also includes an experimental measurement technique using lock-in amplification to remove measurement chain biases however this reduces the maximum sample rate to 10 samples per second.

This module is used for measuring the thrust of the engine and oxidiser mass during hot-fire engine tests. Calibration was performed on this module with load cells for thrust measurement connected resulting in maximum deviation of 0.2% FS for 1000N range.

Capacitance We constructed a cylindrical capacitance sensor for indirect measurement of the level of oxidizer in liquid phase in its tank that is embedded into the tank. It measures the level via change of capacity due to difference in permittivity of liquid and gas N₂O. The sensor is made up from three different capacitors: one referential for gas state permittivity (top ring), one for liquid permittivity (bottom ring) and one for the measurement itself (long tube). All the connections from the sensor to measuring card are shielded from parasitic capacitances so that the measurement is minimally affected by surrounding environment.

The card can handle up to four different capacitors in both differential and single ended measurements. The maximum input range for each channel is 30pF and the resolution 0.5fF. We can offset the incoming value by up to 100pF. The maximum output rate is 400 samples per second. The board communicates with master computer via I₂C protocol.

Thermistor The thermistor module measures temperature data from 16 thermistors. It allows utilization of 4-wire measurement to achieve the best accuracy. The thermistors are fed by two constant current sources. Each current source feeds 8 thermistors. The voltage is amplified via an instrumental amplifier and then digitized with a 12-bit ADC. The ADC communicates with the main measuring system through SPI. Averaging can be applied to further increase accuracy of readings. All channels have been calibrated using a HP 34401A multimeter. After calibration, each channel can achieve an average deviation of around 0.5% FS for Pt1000 thermistor.

Tensometer Tensometric rosette measuring card We are using tensometric rosettes to measure mechanical stress in tanks under pressure during testing. Our measuring card has two channels each consisting of 3 strain gauges. Card can also be configured to measure 6 load cells.

Each strain gauge is powered by a constant current source, so measurements won't be affected by different wire resistances. Power polarity to strain gauges is modulated using H-bridge. Signal is amplified, filtered and measured by a 16-bit ADC. Measurements are taken in both power polarities and subtracted to cancel out op-amp offset voltage. ADC's output is read using SPI at 20 MHz and checked by a CRC to ensure no bit-flip has occurred. Output data rate is 333 Hz when all channels are being used.

One channel of the measuring card can be used to connect a tensometric rosette, which is not attached to a test subject. This rosette can be used to cancel out error introduced by a temperature change.

2.6.3 Flight Software

FC-SW consists of several independent segments, which must accomplish several tasks crucial for successful use CTU Space research rocket. FC-SW must successfully read measured data from onboard sensors and communicate with ground.

Second task is flight commanding of valves and parachutes, which is assured by deterministic state machine. State machine commands rocket based on onboard realtime rocket state estimation like current altitude, speed and acceleration, etc. For live tracking and debugging messaging and logging system was developed. The flight software is written in C language, which is recommended programming language for safety critical applications.

2.6.3.1 Flight software architecture

Flight software consists of several modules. The dataflow diagram can be seen in fig. 2.26. Modules are described in next sections.

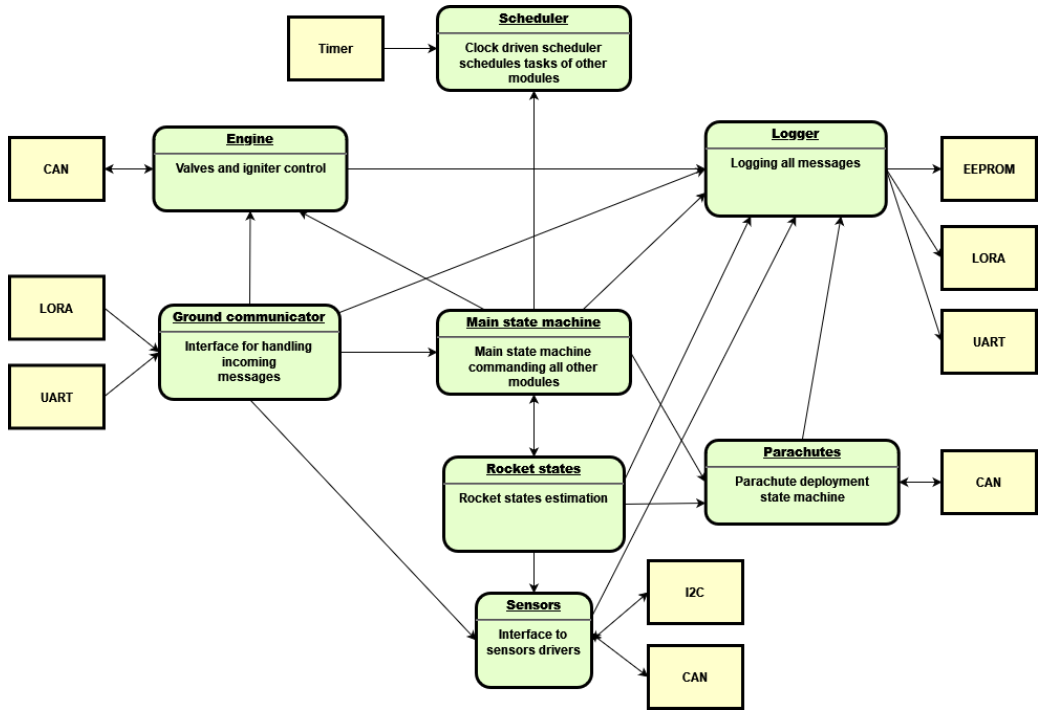


Figure 2.26: Flight software modules dataflow diagram

2.6.3.2 Main state machine

Core of the FC-SW is a state machine which commands flight. Rocket can be in various states during the pre-launch, ascent, descent and landing phases of the flight. We distinguish among several states:

- State configuration
- State armed
- State engine ascent
- State powered ascent
- State unpowered ascent
- State descent
- State landed

The state diagram of the main state machine is in the figure 2.27 Because of complexity of state diagram, we test it in HIL simulation, which we've developed for flight software and flight computer testing.

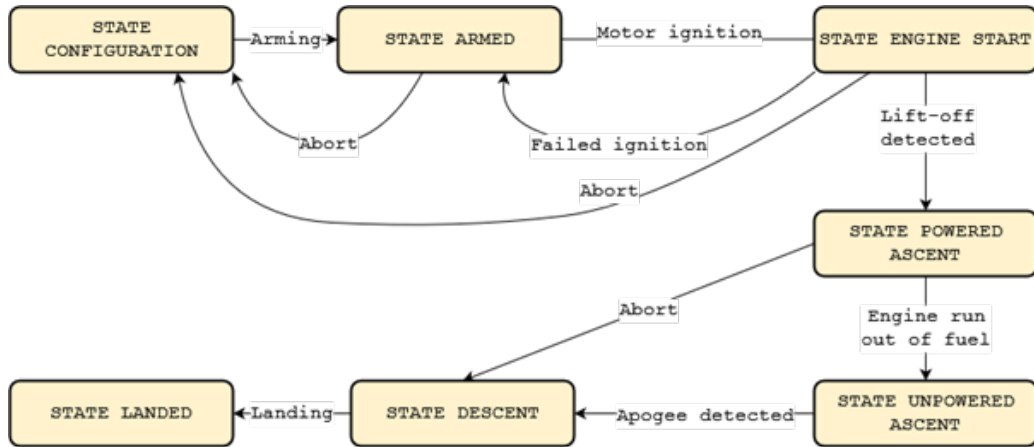


Figure 2.27: Main state machine state diagram

State configuration Rocket is in this state during the pre-launch phase on ground. Ground crew responsible for avionics runs tests of FC-SW by ground station application and complete flight software checklist. Flight computer communicates with ground crew primarily by cable. In this state can user test valves for engine and tanks.

State armed Rocket in this state is armed by software and hardware and the rocket is ready for engine ignition. In this state is possible to disarm rocket at any time and run additional tests or check the rocket hardware.

State engine start In this state rocket waits predefined lift-off countdown until the engine start is detected. Additionally in this state igniter ignition takes place. As is described in logical diagram for engine start. Launch can be cancelled at any time during countdown. Logging of sensors data and rocket states starts.

State powered ascent In this state, rocket engine is supposed to run until the fuel is run out. Thanks to transitions to and from this state we can measure time of engine firing. Knowledge of proper time of engine firing is important for engine model evaluation, thrust characteristics, recovery, etc...

State descent In this state is parachutes state machine evaluated and parachutes are deployed. Rocket descents to ground. The parachute deployment procedure is described in 2.4. When abort occurs, all parachutes are deployed immediately.

State landed In this state rocket waits for recovery and buzzer beeps. Logging is stopped.

2.6.3.3 Rocket states

In this module are rocket states estimated from incoming measurements. States estimations are periodically updated using scheduler. We estimate mainly three states: altitude, vertical speed, vertical acceleration for all transitions among states in the main

state machine and for parachutes state machine transitions. For robustness we use linear stable filters to estimate rocket states.

2.6.3.4 Sensors

In this module are implemented functions and data structures to process and store obtained raw data from sensors. This module is capable to communicate with sensors and raw data from sensors can be logged. This module translates different data format from sensors manufacturers to defined data structure which is general for all sensors of some type(barometer, accelerometer, etc...).

2.6.3.5 Parachutes

Parachutes module implements separate state machine, which is started after apogee detection or abort during launch. This module takes data from rocket states module and log the state machine state. The implementation of the state machine can be found in the figure 2.28.

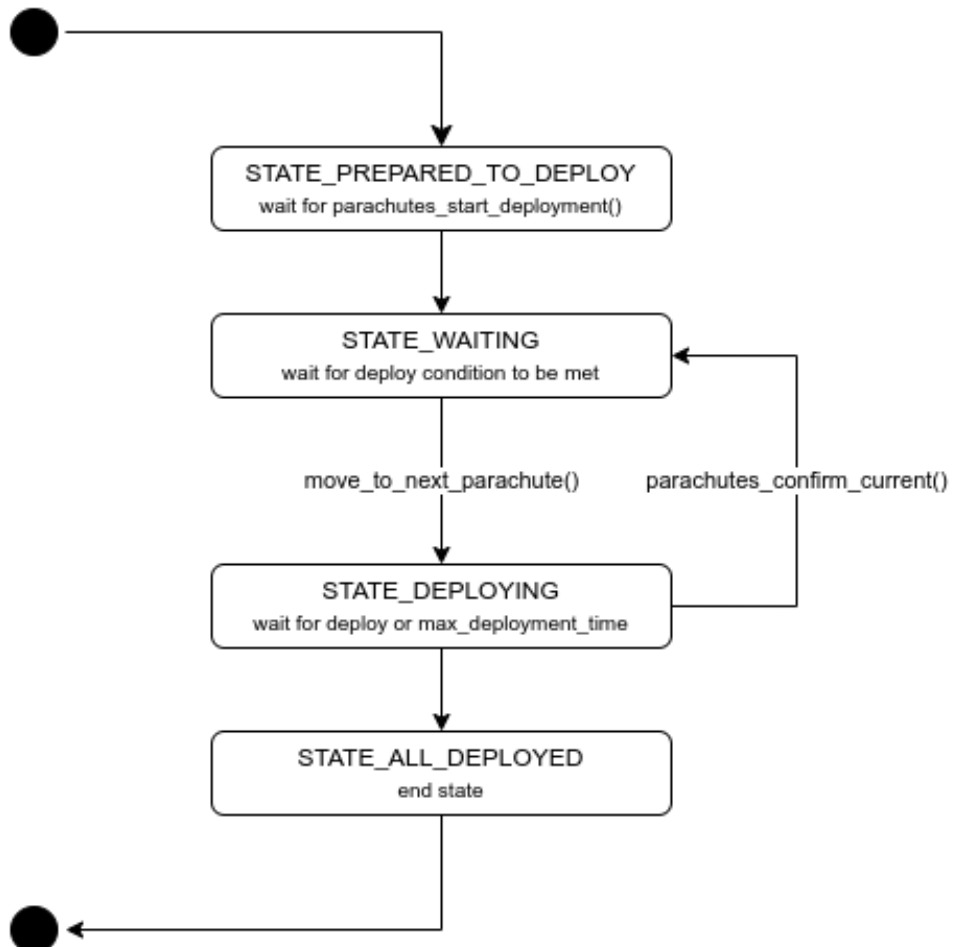


Figure 2.28: Parachutes deployment state machine

Function parachutes confirm current returns true when the parachute deployment is confirmed by an ADC or the is a timeout occurred (we are not sure if the parachutes was deployed by hardware). In the case that abort event occurs, all parachutes are deployed immediately.

2.6.3.6 Logger

Logger module implements functions and structures to store data and it writes data to peripherals as asynchronous event. For each peripheral we use one instance of logger data structure. Each instance has its own queue to store data. Logger uses same data format for logged messages as ground communicator module. On Euroc 2023 we use logger for telemetry data sending to ground station, storing data to EEPROM memory and for debug purposes.

2.6.4 Ground communicator

This module implements functions for processing incoming messages from Lora or debug serial port. New received messages are stored into queue, which is popped as asynchronous event, with exception of the abort event. Ground communicator also parses messages and checks CRC of messages.

Also, this module has some helper functions for making communication protocol message which uses logger module.

2.6.5 Engine

Engine module implements functions to control valves and igniter. It behaves like rocket engine driver and simplifies work with engine for the main state machine.

2.6.6 Scheduler

Scheduler module has implemented clock-driven scheduler, which suits safety critical applications. It has also implemented structure for task which has to be scheduled. In the flight software we use these tasks for sensor measurements, state estimation, logging, state machines evaluations.

2.7 Ground Station

The main role of ground station is communication with rocket and real-time telemetry data processing. Communication with rocket means that we are able to receive incoming messages for rocket but we are able to send commands to the rocket.

We decided to use distributed system with star topology for our ground station. We have one node server, which receives all packets via UDP and sends them to the ground segment of wireless communication segment. This node also streams received messages from rocket as UDP packets to the nodes of the net. Then it is possible to

connect laptop to the network and anyone with access can run own application which process data or send commands. This system enables us to spread work effort among team members to have multiple simple applications, for commanding, data plotting, etc...

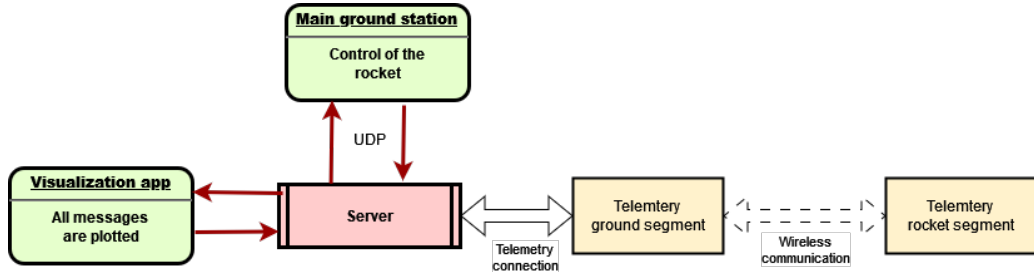


Figure 2.29: Ground station dataflow diagram

2.7.1 Mission control application

This application is programmed in MATLAB. This application has features to send command to the rocket, show basic telemetry data and abort the flight. This application will be used during the launch by an operator. This application has console and GUI available for user. Application shows us current parameters setup of the rocket int table and we can simply compare them with the desired value.

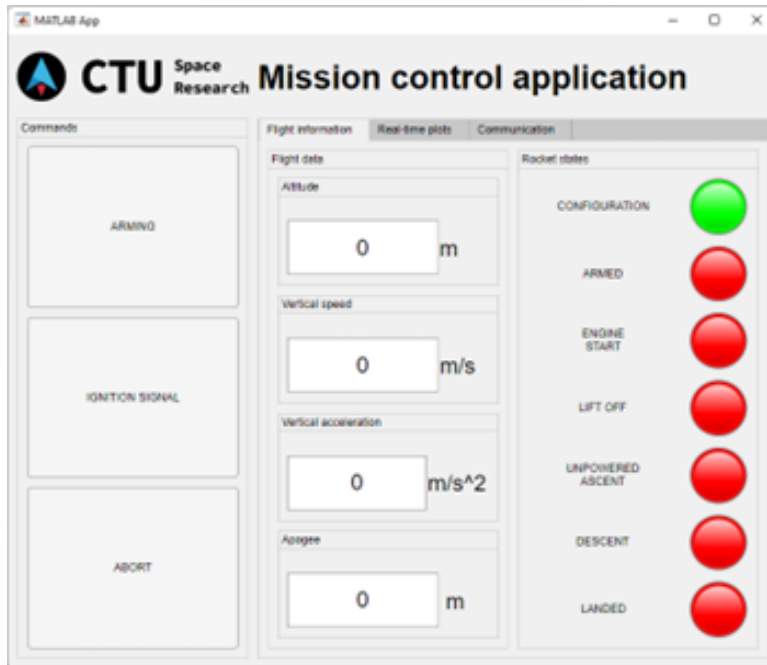


Figure 2.30: Screenshot of mission control application

2.7.2 HIL Simulator

For testing and simulation close to the real launch conditions we have developed HIL(Hardware in the loop simulation) tool. This application uses the Mission control application to command simulated rocket and receive telemetry. Rocket is modelled

in Simulink and communicates with MATLAB via UDP packets on local computer. This simulator helps us to debug flight software without need to have a lot of test flights and test real flight computer.

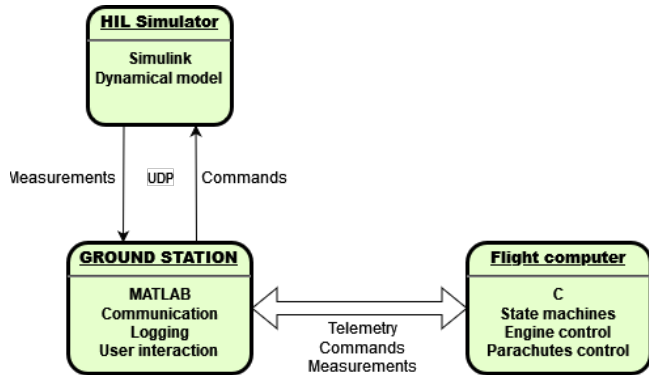


Figure 2.31: Dataflow diagram for HIL testing

2.8 Ground Support Equipment

Refueling of the rocket is handled by a series of electronically controlled ball valves rated at 300 bar. For budget reasons the electronical control system was made inhouse. The system uses a 12V DC automotive engine with internal worm gear assembly to drive a set of 3D printed (PETG material) gears which are connected to the valve. Gear ratio of said external gear assembly is 3:1. The drive gear is secured on the splined conical shaft of the engine using a M8 nut. The conical mating surface of the gear mount is made smaller than the shaft. This results in the splines cutting into the softer plastic material creating a stronger connection, however this means that the gear mount has to be replaced if the system gets disassembled. The total gear ratio allows the system to produce roughly 30 Nm of torque and is able to open/close the valve in circa 2-3s. Failure safety is provided by a set of 2 manually removable pins, which disengage the drive gear from the engine, and by adding levers so the valves can be rotated manually. This allows the user to manually close the valve using the attached handle. The whole system doesn't feature position control and operates only in an open/close mode. This is achieved by 2 adjustable endswitches that are engaged when the valve is in desired position. Power draw of the system is not expected to exceed 75W at peak usage.

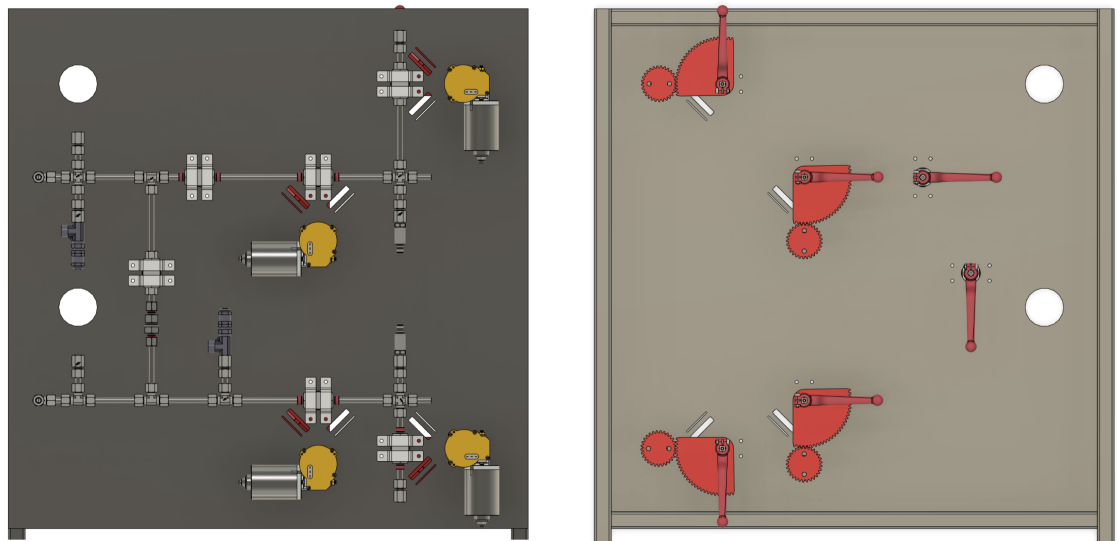


Figure 2.32: Back (left) and front views of GSE

3 Mission Concept of Operations Overview

3.1 Concept of Operations

In order to launch the rocket at the EuRoC competition in Portugal we have decided to split the members coming to the competition into two groups.

The first group going by cars from the Czech Republic is responsible for transporting the rocket to the EuRoC area. This group consists mainly of the core team members so they can oversee in person the packing of a rocket and all of its parts.

Before leaving Prague there will be conducted an integration test which consists of putting the rocket together. Without delay, we will put all the parts into transport boxes and load them into cars. This process will guarantee that we will have all of the components and necessary equipment. For better clarity of the *Concept of Operations* (ConOps) see table 3.1.

Timing	T - 5 weeks	T - 2 weeks	T - 1 week	T - 2 days	T - 1 day	T - 6 hours	T - 3 hours	T - 1 hour	T = 0
Task	Final report	Integration tests + packing	Shipping	Assembly and verifications	Flight Readiness Review	final integration	Launch Readiness Review	Installation on the launch pad	Lift-off

Table 3.1: Pre-flight ConOps

Timing	T + 30 min	T + 1 hour	T + 2 hours	T + 3 hours	T +12 hours	T + 1 day	T + 4 days	T +1 week
Task	Ground recovery	rocket inspection	Post-Flight Review	Rocket Disassembly	Flight Data Analysis	Operations Debrief	Packing + Shipping	Rocket Detailed Analysis

Table 3.2: Post-flight ConOps

Once the team is present in the area, the departments start assembling their modules according to their checklists. The operations are supervised by the Chief Engineer and Group Leaders.

Before heading to the launch area, it is mandatory to pass the Flight Readiness Review (FRR) performed by the EuRoC technical evaluation board.

The team then proceeds to the final integration steps and once the LV is ready, it passes the Launch Readiness Review (LRR), after which the flight card is issued to the team.

The flight unfolds as described in Figure 3.1.1. More detailed ConOps can be found in the Appendices.

Once the rocket is safely recovered, a Post Flight Review (PFR) and a debriefing is done with the jury. The LV is inspected and its condition is recorded. The rocket can then be

disassembled according to the correct procedures.

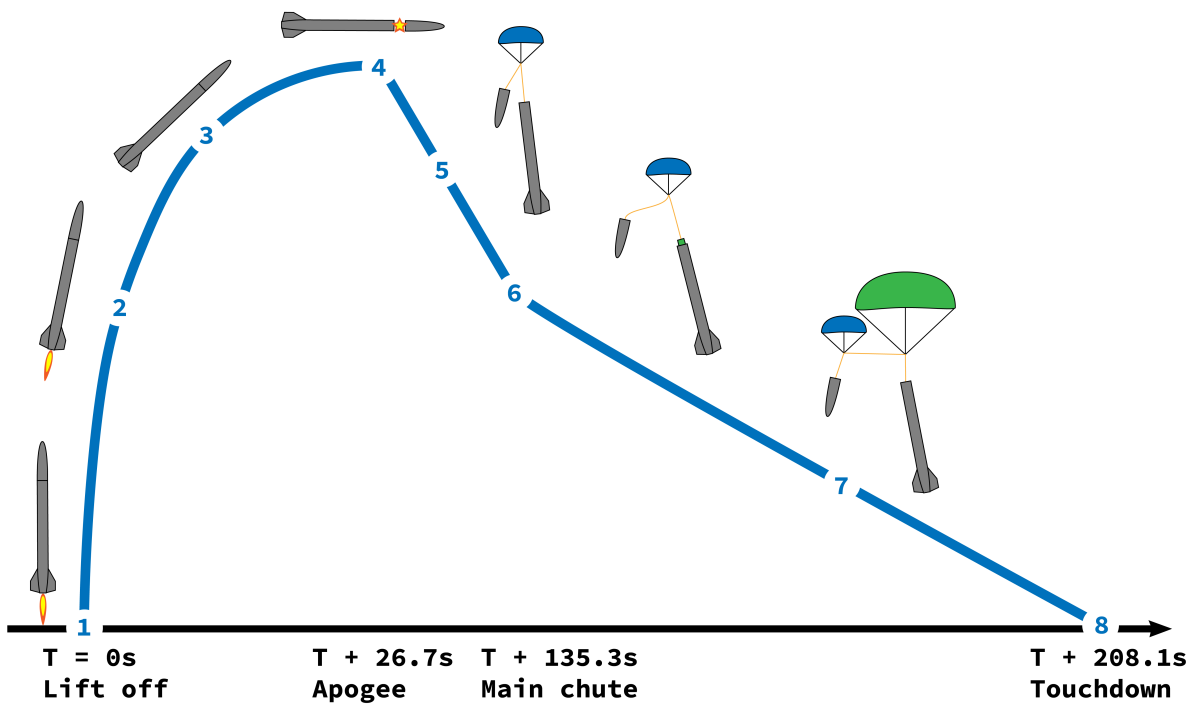


Figure 3.1: Flight ConOps

Phase number	Mission Phase	Time [s]	Main Logic for the Event	Phase Description
0	Arming	-60	All preflight checklists are done and then the software arming signal is sent and confirmed	All preflight checklists are successfully completed and the software ground station sends arming signal to the rocket. Ground station then waits till the arming command is confirmed as received from the rocket's flight computer
1	Liftoff	0	FIRE signal is sent	FIRE signal is sent to the igniter and the main valve from the oxidiser tank is opened with 1 second delay
2	Powered Ascent	0.632	Rocket leaves launchrail	The motor boost lasts until $t + 8$ s, with the rocket reaching maximum velocity of 258.7 m/s
3	Unpowered Ascent	8	Engine burnout	After motor burnout the rocket decelerates due to aerodynamic drag
4	Nosecone Separation	26.66	Apogee Detected	At the recognition of the apogee (vertical speed detected by barometer is negative) the nosecone ejection system is activated and the nosecone is ejected along with the drogue parachute, which begins to unfold
5	Drogue Descent	27.86	Drogue parachute is fully deployed	The drogue parachute is completely deployed and it slows down the rocket to XXX m/s
6	Main Chute Release	135.32	Detection of 450 m altitude	The 3 rings system arming main parachute is activated and the drogue parachute pulls the main parachute out of the rocket, which then begins to unfold
7	Main Descent	137.2	Main parachute is fully deployed	The main parachute is completely deployed and slows down the rocket to 6 m/s
8	Landing	208	The rocket lands	The rocket lands and the recovery procedure begins

Table 3.3: Flight ConOps

3.2 Flight Performance

Flight Performance can be seen in the following table.

Parameter	Value	Unit
Predicted Apogee	3221.792	[m]
Aerodynamic Stability	1.509	[cal]
Centre of gravity	2132	[mm]
Centre of pressure	2374	[mm]
Launch rail exit velocity	30.458	[m · s ⁻¹]
Max Velocity	258.701	[m · s ⁻¹]
Max Acceleration	80.075	[m · s ⁻²]
Drogue descent rate	24.655	[m · s ⁻¹]
Main Parachute descent rate	6.026	[m · s ⁻¹]
Predicted Ground Hit Velocity	6.026	[m · s ⁻¹]

Table 3.4: Flight performance overview

3.3 Trajectories and flight scenarios

The rocket may experience following scenarios, resulting in different trajectories:

- **Nominal flight:** Expected flight scenario. The drogue parachute is deployed at apogee. The main parachute opens at 450 m AGL, slowing rocket enough to enable soft landing.
- **Main parachute deployed at apogee:** Due to slow descent rate the rocket would have in this scenario, it is possible that the rocket would have high drift, resulting in large landing perimeter. That could be dangerous to civilian infrastructure.
- **Only drogue parachute deployed:** In case of unsuccessful main parachute deployment the rocket would descend only on drogue chute, resulting in high impact velocity. In this scenario the damage or the destruction of the rocket is likely.
- **Ballistic flight:** The nosecone doesn't eject or none of the parachutes opens. Rocket will impact the ground with very high velocity, most probably destroying the rocket.

Every part of the recovery system is designed and tested to minimise the risk of other than nominal scenarios to happen.

For testing purposes, we've developed Hardware-in-the-loop simulator, in which we test our flight software during scenarios mentioned above.

Additionaly our avionics hardware and flight software are capable of detecting, whether parachutes were/were not deployed by our flight computer. This feature enables us to act in real-time and give us a chance to avoid ballistic flight.

3.3.1 Nominal flight

As can be seen in the figure 3.1 the rocket flight can be described by several phases. This is encoded in flight software in the main state machine which commands all software modules of the rocket as can be seen in software description in section 2.6.3.1. In each state we have prescribed behaviour of the flight software.

3.4 Flight events

During the flight for correct functionality of main state machine we have to detect events which divide state machine states. Events are described in the following subsections.

3.4.1 Arming detection

Our rocket can be armed manually and by software. This feature increases safety of the ground crew preparing the rocket for flight. In dangerous situations rocket can be disarmed wirelessly by the operator or ground crew manually. For arming the rocket this double arming ensures better safety of the ground operations.

After all successful checklists a set software arm message is sent to the rocket. After receiving this message flight computer replies, that is armed. Than we can start tanking procedure described in appendix.

3.4.2 Lift-off detection

Mentioned in the section 2.6.3.3 we estimate vertical acceleration of the rocket. Using estimated acceleration in the body coordinate system we are able to detect lift-off and successful engine ignition. Other way how to detect launch is significant increase in altitude. We combine these both conditions with logical or operator. This detection is turned on only after the end of the pre-launch countdown. This function protects us from an unwanted change in the state of the main state machine, for example while manipulating with the rocket.

3.4.3 Engine burnout detection

Engine burnout divides powered and unpowered ascent states of the rocket flight. This event can be detected by looking at the jerk or sign of rocket body acceleration. Information about this event provides us the time of engine firing and we can detect some problems with propulsion subsystem. Using simulation and burn time we are able to estimate the place, where rocket is going to land.

3.4.4 Apogee detection

Apogee is detected by evaluating rocket vertical speed. Vertical speed has opposite sign than velocity v_z in z axis of the rocket's NED(north-east-down) coordinate system. Vertical velocity is estimated by highpass filtering the barometric altitude.

In order to prevent detecting apogee in ascent phase of flight the sing of vertical velocity is validated for 1 s since the first detection of negative speed. This ensures that the rocket has reached apogee and descends.

3.4.5 Landing detection

Landing of the rocket is detected by barometric altitude. When rocket is near the ground in 10 m a landing event is detected.

3.5 Deployment events

During nominal flight two deployment events for drogue and main parachute are planned. Parachute deployment is implemented in another state machine for parachutes. Each parachute has various states representing the actual state of deployment, which are described in section 2.6.3.5.

4 Conclusions and Outlook

In the two years that the team has been in operation, we have managed to build the basic team infrastructure from the ground up, including the team management system, acquiring meeting and production space, and gaining support from sponsors, which is a clear signal to us that we are on the right track. The production of the rocket and all of its subsystems presented a series of challenges for the team, but the team has successfully managed the basic level of production. However, the progress of the development has definitely not been optimal and we have a big series of challenges to go through before next year.

There is a need to improve collaboration between the different groups, and the personal distribution of the roles of team leader and systems engineer should definitely contribute to this. More emphasis will be placed on the implementation of systems engineering, which has not been given enough space this year due to the inexperience of members with group projects. This will improve the documentation issues, or overseeing the ongoing development, and the timing of the development and validation process. The team had no experience with such issues.

Unfortunately, there are problems that are beyond resolution - the payload group consisted mostly of international students from Ukraine who were headed to their home country for the holidays, where they had other concerns for obvious reasons. Hence the change of mission from experiment to ballast. For next year, we need to prepare for such situations as well.

A lesson learnt from this year is also for the team and group leaders to take personal responsibility, when the issue of production of some components of the rocket was held up until the review call with the EuRoC judges, which led to delays in production.

The overall plan for the next year is to build on the Illustria design to develop a new rocket that will retain the basic characteristics, but there will be an overall lightweighting and improvement in the functionality of all components without adding critical points to the functionality of the rocket.

One of our team's goals was to get more students interested in STEM fields. The increasing number of team members and successful undergraduate and graduate theses in our team is proof that we are succeeding in this goal. We hope that Illustria's presence at our student events will attract even more interested and enthusiastic students to the space.

All team members have put a lot of effort and dedication into getting the Illustria project and the team to the point it is at now. This gives confidence that the whole team

will continue to progress at the same pace into the next years of the European Rocketry Challenge.

5 Appendices

5.1 System Data

Parameter	Value	Unit
Flight Category	H3	[-]
Propulsion type	SRAD Hybrid	[-]
Length	3520	[mm]
Diameter	161	[mm]
Total Launch Mass	28.817	[kg]
Number of fins	3	[-]
Stability off the rails	1.509	[cal]
Launch rail exit velocity	30.458	[m · s ⁻¹]
Predicted apogee	3221.792	[m]
Predicted max acceleration	80.075	[m · s ⁻²]
Predicted max velocity	258.701	[m · s ⁻¹]
Predicted Flight Time	208.128	[s]

Table 5.1: General Specifications

Parameter	Value	Unit
Total Impulse	9035.37	[N · s]
Maximum Thrust	1849.36	[N]
Average Thrust	1079.49	[N]
Burn Time	8.37	[s]
Launch Mass	3.7	[kg]
Dry Mass	2.4	[kg]
Fuel	ABS	[-]
Oxidiser	N ₂ O	[-]
Pressuriser	N ₂	[-]

Table 5.2: Engine Specifications

Parameter	Value	Unit
Drogue Chute Diameter	700	[mm]
Drogue Chute Drag Coefficient	1.45	[$-$]
Drogue Chute Deployment Velocity	21.875	[$m \cdot s^{-1}$]
Main Chute Diameter	2800	[mm]
Main Chute Drag Coefficient	1.45	[$-$]
Main Chute Deployment Velocity	24.655	[$m \cdot s^{-1}$]
Main Chute Deployment Altitude	450	[m]
Predicted Ground Hit Velocity	6.026	[$m \cdot s^{-1}$]

Table 5.3: Recovery Specifications

Parameter	Value	Unit
Battery Voltage	7.4	[V]
Battery Type	Li-Ion 18650	[$-$]
Battery Capacity	3400	[mAh]
Endurance	6	[hours]
RF Protocol	LoRa	[$-$]
Maximum RF Transmission power	100	[mW]
Tested range	1000	[m]
Estimated maximum range	10000	[m]
RF frequency	865-870	[MHz]
Rocket Antenna Type	Omnidirectional	[$-$]
Rocket Antenna Gain	-5	[dBi]
GCS Antenna Type	Omnidirectional	[$-$]
GCS Antenna Gain	-5	[dBi]
Maximum Bit Rate	2	[kbps]

Table 5.4: Electronic Specifications

5.2 Detailed Test Reports

THIS PAGE IS INTENTIONALLY LEFT BLANK



RECOVERY SYSTEM GROUND TEST

Prepared by: Jakub Hajný, Aleš Zapadlo

Checked by: Klára Čepová

Approved by: Přemysl Čechura

Date: 10. 09. 2023

I Introduction

The objective is to test the nose cone ejection in the horizontal position, which we consider as the worst case scenario.

I-A Goal of the test

The goal of this ground test is to prove the ability of the SRAD recovery system to successfully eject the nose cone therefore deploy the drogue chute. This test is only considered successful if the nose cone is fully ejected and detached from the rocket body.

II Testing process

To test the functionality of the SRAD recovery system, we attach the recovery section prototype containing the recovery system to the rocket body prototype (a piece of GFRP tube with appropriate dimensions). This assembly is then firmly fixed to support. Both flight computers are hidden inside the GFRP tube, which provides them protection during the test. The nose cone prototype is filled with parachutes and lines in flight configuration and then placed on the recovery section. After this preparation, the E-matches in the SRAD Pyro Valves can be armed allowing the test to be performed.

II-A List of Equipment

List of equipment:

- Nose cone prototype (NSP)
- Rocket body prototype (RBP)
- Recovery section prototype (RSP)
- Parachutes and lines in flight configuration
- SRAD recovery system (2x SRAD Pyro Valve, 2x CO₂ cartridge)
- Voltage source
- Cimrman Flight Computer
- Vega Flight Computer
- Ground support

II-B Test Procedure

Step by step test procedure.

1. Mechanically arm the Pyro Valves with black powder and E-matches
2. Assemble the Pyro Valves and the CO₂ cartridges
3. Mount the Pyro Valves with CO₂ cartridges to a plate in the RSP
4. Attach the RSP to the RBP
5. Firmly attach this assembly to the ground support
6. Pack all the parachutes and lines into the NSP
7. Place the NSP on top of the grounded assembly
8. Connect both flight computers
9. Electrically arm the E-matches in the Pyro Valves
10. Retreat to a safe distance
11. Actuate the mechanism
12. Observe the result, check for any damage

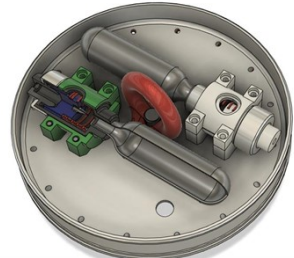


Figura 1. Packaging layout on recovery RADAX

III Testing

The test was carried out without any major problems. The first time, there was a bad connection between the E-matches and the flight computers. Once the error was corrected, the test was successful.

IV Conclusion

In this test we successfully managed to prove the ability of the SRAD recovery system to fully eject the nose cone in the worst case scenario



Figura 2. Recovery System Prototype



Figura 3. Testing Setup



Figura 4. Testing Setup After Ejection

position. Both cartridges were pierced as intended. There was no visible damage done to the parachutes nor other components.



Propellant loading and off-loading test

Prepared by: Daniel Hořejší

Checked by: Jakub Zeman

Approved by: Lukáš Mičan

Date: 30. 08. 2023

I Introduction

For the safe start of the rocket it is important to safely load and in the case of emergency off-load the oxidizer. For this reason a test of loading and off-loading oxidizer was performed. The pressurizer gas and oxidizer liquid are the same as the ones that are planned to be used in the rocket (N_2 for pressurizer and N_2O for oxidizer). The fluid system is divided into two section via servo valve. The low-pressure section contains the oxidizer tank and the high-pressure section contains the pressurizer gas.

II Testing process

The goal of the test is to ensure that the oxidizer can be safely loaded and than off-loaded through the engine. The test is considered successful if the entire process is carried out without any unplanned physical intervention during the test.

II-A List of Equipment

List of equipment:

- substation
- oxidizer tank
- pressurizer tank
- ground support (valve control, oxidizer and pressurizer tank weight and pressure monitoring)
- pressurizer supply tank
- Oxidizer supply tank

II-B Test Procedure

Step by step test procedure.

1. Assemble the testing aperture
2. Test every servo valves in the aperture (move to open and closed position)
3. Test the main valve (open and close the valve)
4. Connect pressure sensors and begin recording and monitoring the pressure
5. Begin monitoring tank weight

6. Clear the immediate area around the aperture and close all valves and move servo valves to closed position
7. Pressurize high pressure section to test pressure of 90 bar
8. Open servo valve between high-pressure and low-pressure section - wait for pressure to equalize
9. Close servo valve between high-pressure and low-pressure section
10. Pressurize high pressure section to 180 bar
11. Open servo valve between N_2O supply tank and low-pressure section - wait for pressure to equalize
12. Close servo valve between N_2O supply tank and low-pressure section
13. Open servo valve between oxidizer tank and outer atmosphere to vent the gas on top of liquid N_2O
14. Repeat steps 11 and 13 three more times
15. Open servo valve between high-pressure and low-pressure section - wait for pressure to equalize
16. Open valve to went the oxidizer

III Testing

The test was carried out without any unplanned intervention and is therefore considered to be successfull.

IV Conclusion

The test proved the ability to safely load and off-load the oxidizer from the oxidizer tank.

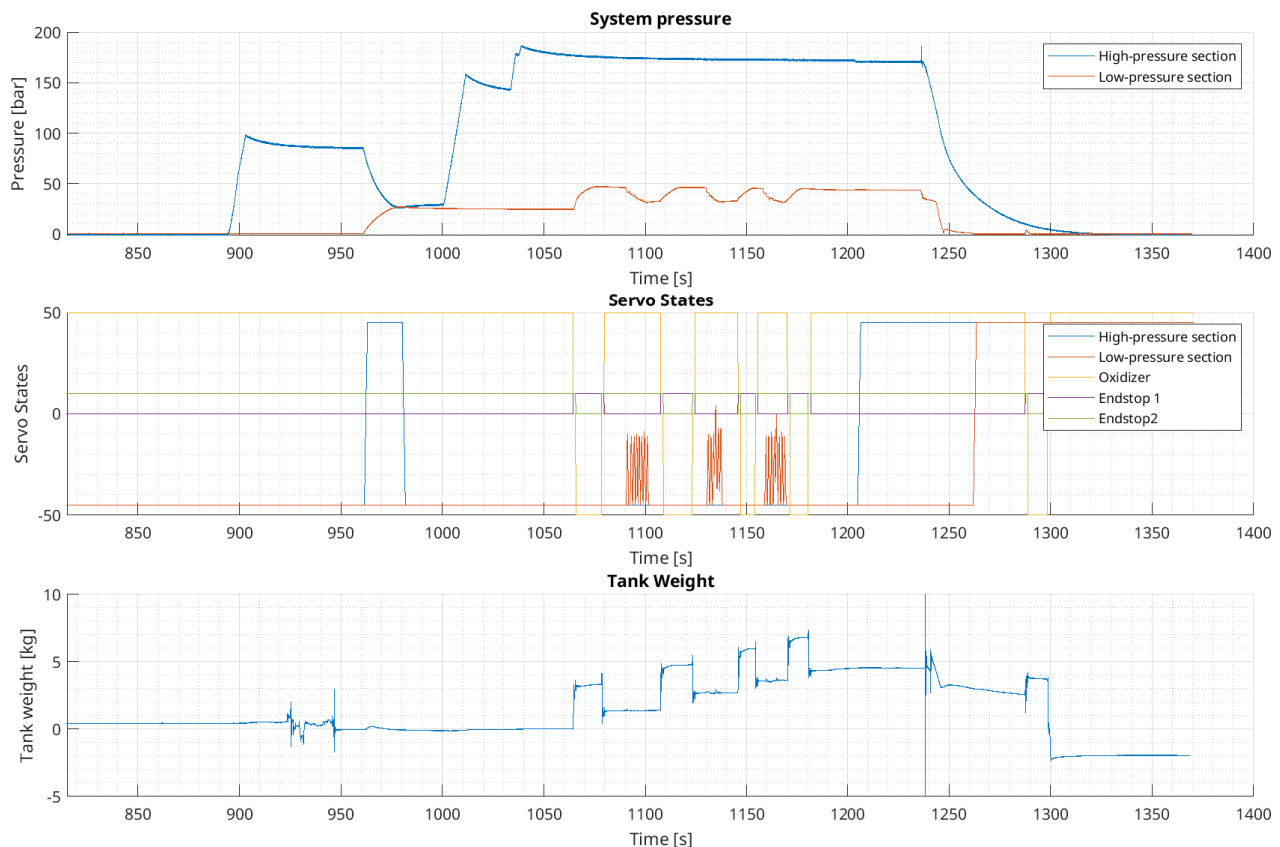


Figura 1. Propellant loading and off-loading



Figura 2. Propellant loading and off-loading



Test of SRAD flight computers with capability of actuating the recovery systems

Prepared by: Aleš Zapadlo
Checked by: Dominik Beňo
Approved by: Lukáš Mičan
Date: 06. 09. 2023

I Introduction

The objective is to test the capability of SRAD flight computer to actuate the recovery system including flight state detection. The flight computer will be tested to prove correct detection of flight stages and the ability to perform actions based on that.

II Testing process

To test the functionality of the SRAD flight computer to detect flight stages correctly, a HIL (hardware-in-the-loop) simulation is used. The HIL simulation provides sensor data to the flight computer based on a model. The flight computer processes the simulated sensor data and performs action based on estimated state. The flight computer is connected to the recovery system - both nose cone ejection system and three-ring mechanism. When flight computer estimates the rocket is in apogee it deploys the nose cone and drogue chute. After descending to the target altitude of 450m it deploys the main chute by activating the three-ring mechanism.

II-A List of Equipment

List of equipment:

- SRAD Flight Computer Cimrman Mini V3
- Nose cone and drogue chute ejection system (2x SRAD Pyro Valve, 2x CO₂ cartridge)
- Three-ring mechanism with E-matches
- Flight computer battery
- Computer with HIL simulation
- USB-to-UART converter

II-B Test Procedure

Step by step test procedure.

1. Mechanically arm the Pyro Valves with black powder and E-matches

2. Assemble the Pyro Valves and the CO₂ cartridges
3. Assemble the three-ring mechanism with E-matches
4. Connect the nose cone and drogue ejection system to the flight computer
5. Connect the three-ring mechanism to the flight computer
6. Connect flight computer to the HIL simulation computer with USB-to-UART converter
7. Connect battery to the flight computer
8. Arm the flight computer
9. Retreat to a safe distance
10. Activate simulation
11. Observe the result

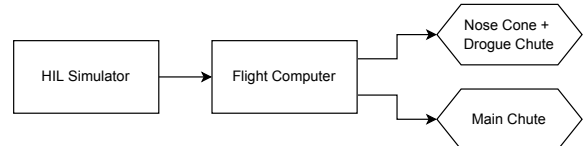


Figura 1. Test connections diagram

III Testing

The first attempt of the test was aborted due to bad connection to the pyro valve E-match. This issue was detected by the onboard continuity test and was corrected before the HIL simulation was started. The second attempt was carried out without any major problems.

IV Conclusion

The flight computer correctly detected the flight stages and deployed both parts of the recovery system. The nose cone and drogue chute were correctly activated after reaching the apogee. The main chute was deployed after detecting the altitude of 450m.

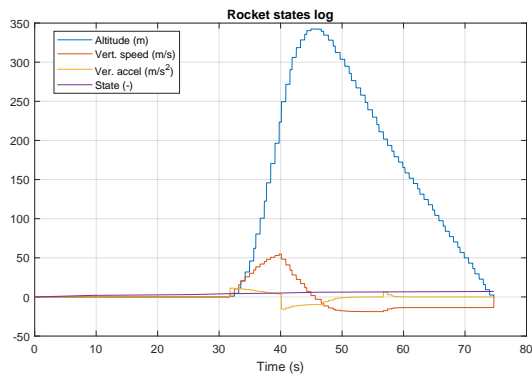


Figura 2. HIL Simulator output

```
LOG_STATE_MSG: Time: 9.515. State ARM.  
LOG_STATE_MSG: Time: 25.628. State ENGINE_START.  
LOG_ENG_CTRL_REG: Time: 30.633. Eng.ctrl.reg: 1  
LOG_STATE_MSG: Time: 30.633. State LIFT_OFF.  
LOG_STATE_MSG: Time: 40.134. State UNPOWERED_ASCENT.  
LOG_STATE_MSG: Time: 45.643. State DESCENT.  
LOG_MSG_PARACHUTES_NEW_STATE: Time: 45.693. Index: 0. State: STATE_WAITING  
LOG_MSG_PARACHUTES_NEW_STATE: Time: 45.744. Index: 0. State: STATE_DEPLOYING  
LOG_MSG_PARACHUTES_NEW_STATE: Time: 46.744. Index: 0. State: DEPLOY_FINISHED_DUE_TO_TIME  
LOG_MSG_PARACHUTES_NEW_STATE: Time: 46.744. Index: 1. State: STATE_WAITING  
LOG_MSG_PARACHUTES_NEW_STATE: Time: 56.009. Index: 1. State: STATE_DEPLOYING  
LOG_MSG_PARACHUTES_NEW_STATE: Time: 59.009. Index: 1. State: DEPLOY_FINISHED_DUE_TO_TIME  
LOG_MSG_PARACHUTES_NEW_STATE: Time: 59.009. Index: 2. State: STATE_ALL_DEPLOYED  
LOG_STATE_MSG: Time: 74.698. State LANDED.
```

Figura 3. Flight Computer logs



PYRO VALVE TEST

Prepared by: Jakub Hajný
Checked by: Vojtěch Ježek
Approved by: Přemysl Čechura
Date: 30. 08. 2023

I Introduction

The objective of this test is to prove the functionality of the SRAD Pyro Valve.

I-A Goal of the test

The aim of the test is to find the ideal amount of black powder required for successful perforation of the CO₂ cartridge. This test can be declared successful only when the CO₂ cartridge is pierced.

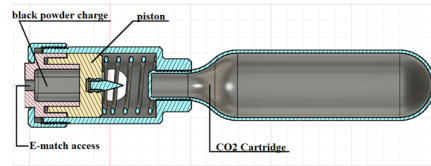


Figura 1. Pyro Valve Design

II Testing process

To test the appropriate amount of black powder in the pyro valve, we started with the smallest value we could weigh, 0,11 g. Gradually, we increased the value up to 0,20 g, at which point the cartridge was successfully perforated.

Each Pyro Valve is actuated by an E-match from a safe distance.

II-A List of Equipment

List of equipment:

- Clamp
- Kitchen Scale
- SRAD Pyro Valve
- 20 g CO₂ Cartridge
- E-match (2 pcs per one Pyro Valve)
- Black Powder
- LiPo Battery



Figura 2. Pyro Valve Test

II-B Test Procedure

Step by step test procedure.

1. Insert 2 E-matches into the Pyro Valve
2. Weigh exact amount of Black Powder (0,11 g first iteration – 0,20 g last iteration)
3. Pour black powder into the Pyro Valve
4. Assemble the Pyro Valve and the CO₂ cartridge
5. Hold the mechanism in place with a clamp
6. Retreat to a safe distance
7. Actuate the E-match
8. Observe the test result
9. Repeat the procedure with increased amount of black powder

IV Conclusion

We managed to successfully test SRAD Pyro Valve and its capability to pierce the CO₂ cartridge. For sufficient safety of the launch, we set the final amount of black powder at 0,3-0,4 g.

5.3 Hazard Analysis Report

Material / Component	Potential Hazard	Mitigation	Level of Risk
Oxidiser	Leakage, frostbites to the personnel	The rocket will be powered by a remotely controlled GSE. All GSE fluid components will be pressure tested in advance.	Low
Black Powder	Unintended combustion	Safeguarded within a certified, fireproof container at all times before utilization, while all sources of ignition will be stored in distinct containers.	Medium
E-matches	Accidental ignition causing fire or burns to personnel	E-matches should only be connected to tested firing systems that require multiple deliberate actions to activate. They will be handled only by authorised person.	Low
Ignitors	Accidental ignition causing fire or burns to personnel	Safeguarded within a certified, fireproof container at all times before utilization, while all sources of ignition will be stored in distinct containers. E-matches will be installed only prior to final assembly.	Low
LiPo Batteries	Fire caused by overcharge, overdischarge or puncture	To prevent potential problems, batteries will undergo charging with suitable chargers. For multi-cell batteries, a balance charging procedure will be implemented to eliminate any risk of overcharging individual cells. When dealing with batteries, it's essential to exercise caution and refrain from using sharp tools that could puncture the cells. Furthermore, all wiring will undergo meticulous soldering and insulation to minimize the chances of short circuits.	Low

Table 5.5: Hazard Analysis

5.4 Risk Assessment

Risk assessment was done in accordance with FMECA approach. The likelihood of a failure mode occurrence and the severity of the occurrence is assigned values according to the following tables:

Failure Probability	Value	Assessment of Risk
Remote	1	This is unlikely to happen
Occasional	2	This might happen
Probable or likely	3	This is likely to happen

Table 5.6: Likelihood of failure

Mishap Severity	Value	Effect of Failure Mode
Minor or negligible	1	Minor impact on mission
Critical	2	Deterioration of performance and mission
Catastrophic	3	Safety hazard and/or likely loss of mission

Table 5.7: Severity of Occurrence

Criticality Ranking	Overall Impact	Severity of Need for Attention/Mitigation
1	Minor	This failure mode is not a concern
2	Minor	This failure mode is of very minor concern
3	Medium	Justification needed. Jury may decide to review
4	High	Technical jury approval needed before launch
6	Critical	Action required to reduce ranking before launch
9	Critical	Action required to reduce ranking before launch

Table 5.8: Criticality ranking

5.4.1 General

Failure Mode	Mission Phase	Failure Probability	Mishap Severity	Criticality Ranking	Team Comments and Justification
Wind gust at launchpad exit causing the rocket to tilt from nominal trajectory	Liftoff	1	2	2	The rocket's aerodynamic surfaces are designed to grant a maximum stability margin of 2 calibers at launchrail exit, preventing the rocket alignment with the wind for high gust speed.
The thrust of the motor is lower than the nominal one causing low exit velocity at launchpad. Rocket drifts from nominal trajectory due to high angle of attack	Liftoff	2	2	4	Hybrid motor is SRAD, but thoroughly tested. The motor is slightly overpowered, so slightly-lower-than-nominal thrust shall still ensure safe liftoff. Team will continue on improvement on thrust prior to EuroC, according test reports will be added.
The thrust of the motor is higher than the nominal one causing apogee overshoot.	Powered flight	2	1	2	Hybrid motor is SRAD, but thoroughly tested. Still some irregularities might happen, but the only result will be missed target apogee. No safety concern is involved.
Damage to the rocket during transport	Transport to Portugal	1	3	3	Each of the rocket's modules does have its own custom-fitted transportation box. Members of the team will be transporting the boxes overseeing the process

Table 5.9: General criticality ranking

5.4.2 Propulsion

Failure Mode	Mission Phase	Failure Probability	Mishap Severity	Criticality Ranking	Team Comments and Justification
Motor assembly error	Assembly	1	3	3	Motor integration rehearsal
Motor manufacturing defect	Pre-flight	1	3	3	The engine is thoroughly tested before testing and launch
Oxidiser tank structural failure	Pre-flight	1	3	3	The oxidiser tank is thoroughly tested before testing and launch
Fluid system leakage	Pre-flight	1	2	2	Fluid system integration rehearsal. Pressure test during integration.
Main valve won't open	Liftoff	2	2	4	Igniter will burn off in 5 seconds, no harm done. Better connectors to the main valve are in manufacturing process

Table 5.10: Propulsion criticality ranking

5.4.3 Structure

Failure Mode	Mission Phase	Failure Probability	Mishap Severity	Criticality Ranking	Teams Comments and Justification
Fins misalignement	Manufacturing	1	2	2	Mold for laminations were designed to serve as an alignment jig at the same time
RADAX couplers failure	Flight	1	3	3	Careful design, manufacturing and integration process
Motor mount failure	Powered Flight	1	3	3	Careful design, manufacturing and integration process
Inner load bearing structure failure	Flight	1	3	3	Designed with generous safety margin to withstand loads that should not occur during nominal or slightly-off-nominal flight
Load-bearing hull failure	Flight	1	3	3	Designed with generous safety margin to withstand loads that should not occur during nominal or slightly-off-nominal flight
Damage during transportation to the launch pad	Pre-flight	1	2	2	The most fragile parts were designed to withstand slight shocks. They still need to be handled carefully

Table 5.11: Structure criticality ranking

5.4.4 Recovery

Failure Mode	Mission Phase	Failure Probability	Mishap Severity	Criticality Ranking	Team Comments and Justification
Nosecone ejection failure	Apogee	1	3	3	System was repeatedly tested and is designed to be redundant, so even one functioning nosecone ejection system working is enough
Parachutes compromised from ejection system explosion	Pre-apogee	1	2	2	Nosecone ejection system is designed so only CO ₂ is venting to nosecone interior
Drogue/Main parachute opening shock cord failure	Descend	1	3	3	Both parachutes have sliders that are designed and tested to reduce their opening speeds, thus reducing shock
Failure of the main parachute cutting system	Descend	1	3	3	The system is redundant and tested
Early parachute deployment	Lift-Off and Ascent	1	3	3	SRAD flight computer is flight-proven to ensure it triggers at correct point in flight
Landing location prohibits rocket recovery	Post-flight	1	2	2	Should not occur with expected (EuRoC approved) launching wind speeds and directions

Table 5.12: Recovery criticality ranking

5.4.5 Flight software

Failure Mode	Mission Phase	Failure Probability	Mishap Severity	Criticality Ranking	Teams Comments and Justification
Software Crash	Pre-flight + Flight	1	3	3	We have a backup COTS flight computer
No apogee detection	Apogee	1	3	3	Critical part, which is tested in HIL
No liftoff detection	Liftoff	1	3	3	HIL testing, altitude or acceleration condition in liftoff detection
Inaccurate state estimation	Flight	1	2	2	HIL tested, we use stable linear filters
Self arming	Pre-flight	1	2	2	Need for a hardware arm
Communication loss	Pre-flight + Flight	2	2	4	Flight computer automatically detects states and deploys parachutes

Table 5.13: Flight software criticality ranking

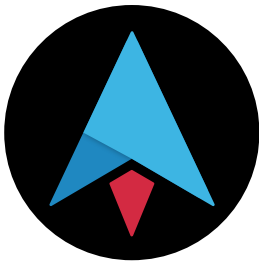
5.4.6 Electronics

Failure Mode	Mission Phase	Failure Probability	Mishap Severity	Criticality Ranking	Team Comments and Justification
Not enough battery charge to launch after wait time on launchpad	Liftoff	1	3	3	The rocket is being charged by the wireless charger while sitting on the launchpad
Recovery system igniter not properly connected	Descend	1	3	3	Igniter electrical continuity testing is implemented in the onboard electronics
Not enough supercapacitor charge to activate any of the recovery sequence	Descend	1	3	3	The recovery system can be activated by the backup flight computer
Rocket main bus connectors disconnecting	Flight	1	3	3	The wiring inside rocket uses connectors with locks
Loss of communication with the GSE	Pre-flight + Tanking	1	1	1	GSE Controller will abort all tanking procedures until communication is reestablished
GPS antenna is in bad orientation after landing and is not able to fix position	Landed	2	1	2	Rocket recovery localization using highly directional antenna or backup flight computer localization will be used

Table 5.14: Electronics criticality ranking

5.5 Checklists

THIS PAGE IS INTENTIONALLY LEFT BLANK



Ilustria



Preflight Checklist

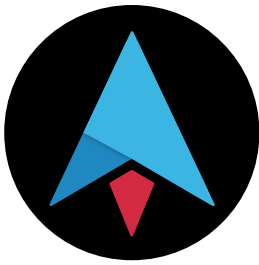
Component: Flight software

Date: _____

Responsible person: Dominik Beňo

#	Item	Check
1.	<u>Check communication</u>	<input type="checkbox"/>
2.	<u>Check flight software version</u>	<input type="checkbox"/>
3.	<u>Logging</u>	<input type="checkbox"/>
4.	<u>Sensors measures correctly</u>	<input type="checkbox"/>
5.	<u>Valves actuation</u>	<input type="checkbox"/>
6.	<u>Check flight software parameters</u>	<input type="checkbox"/>
7.	<u>Ignition detected false</u>	<input type="checkbox"/>
8.	<u>Apogee detected false</u>	<input type="checkbox"/>
9.	<u>Landing detected false</u>	<input type="checkbox"/>
10.	<u>Parachutes state machine state: STATE_PREPARED_TO_DEPLOY</u>	<input type="checkbox"/>
11.	<u>Flight computer is NOT software armed</u>	<input type="checkbox"/>
12.	<u>Flight computer is armed by hardware</u>	<input type="checkbox"/>

Signature: _____



Illustria



Onboard Avionics Pre-flight Checklist

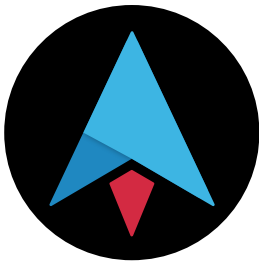
Date: _____

Responsible person: _____

#	Item	Check
1.	Module Management Boards (MMB) in Engine section present	<input type="checkbox"/>
2.	Rocket Bus connected to MMB in Engine section	<input type="checkbox"/>
3.	Main Valve connected to MMB in Engine section	<input type="checkbox"/>
4.	Module Management Boards (MMB) in Pressurizer section present	<input type="checkbox"/>
5.	Rocket Bus connected to MMB in Pressurizer section	<input type="checkbox"/>
6.	High pressure valve servo connected to MMB in Pressurizer section	<input type="checkbox"/>
7.	Low pressure valve servo connected to MMB in Pressurizer section	<input type="checkbox"/>
8.	High Pressure sensor connected to MMB in Pressurizer section	<input type="checkbox"/>
9.	Low Pressure sensor connected to MMB in Pressurizer section	<input type="checkbox"/>
10.	Temperature sensor connected to MMB in Pressurizer section	<input type="checkbox"/>
11.	Module Management Boards (MMB) in Recovery section present	<input type="checkbox"/>
12.	Rocket Bus connected to MMB in Recovery section	<input type="checkbox"/>
13.	Nosecone release system connected to MMB in Recovery section	<input type="checkbox"/>
14.	Main parachute release system connected to MMB in Recovery section	<input type="checkbox"/>
15.	Nosecone release system continuity OK	<input type="checkbox"/>
16.	Main parachute release system continuity OK	<input type="checkbox"/>
17.	Main flight computer present	<input type="checkbox"/>
18.	Rocket Bus connected to main flight computer	<input type="checkbox"/>

-
19. Wireless charger present
20. Rocket bus connected to wireless charger
21. Wireless charger power input connected to main flight computer
22. Wireless charger power output connected to main flight computer
23. Wireless charger umbilical bridge connected to main flight computer
24. GPS antenna connected to main flight computer
25. Telemetry antenna connected to main flight computer
26. Arming board connected to main flight computer
27. Batteries in main flight computer charged
28. Batteries in main flight computer present
29. Backup flight computer present
30. Backup flight computer connected to the nosecone release system
31. Backup flight computer connected to the main parachute release system
32. Backup flight computer telemetry antenna connected
33. Backup flight computer batteries charged
34. Backup flight computer batteries connected
35. Backup flight computer Nosecone release system continuity OK
36. Backup flight computer Main parachute release system continuity OK
37. Main flight computer wireless communication OK
38. Backup flight computer wireless communication OK
39. Igniter present
40. Igniter connected to the UnIO system
41. Igniter contiunity OK
42. Main flight computer armed
43. Backup flight computer armed
44. Igniter armed

Signature: _____



Ilustria



GSE Checklist

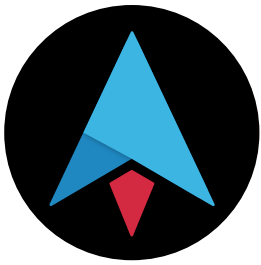
Date: _____

Responsible person: _____

#	Item	Check
1.	GSE fluid systems ready	<input type="checkbox"/>
2.	GSE assembled	<input type="checkbox"/>
3.	UniO System present	<input type="checkbox"/>
4.	UniO Power connected	<input type="checkbox"/>
5.	UniO Ethernet connected	<input type="checkbox"/>
6.	Communication between UniO system and ground station OK	<input type="checkbox"/>
7.	GSE Pressure sensors connected to UniO system	<input type="checkbox"/>
8.	Check pressure sensors data	<input type="checkbox"/>
9.	GSE Valve Motors (4x) connected to UniO system	<input type="checkbox"/>
10.	GSE Valve Endstops (4x) connected to UniO system	<input type="checkbox"/>
11.	Check GSE valves movement	<input type="checkbox"/>
12.	Wireless charger connected to UniO system	<input type="checkbox"/>
13.	Wireless charger holder connected to UniO system	<input type="checkbox"/>
14.	Check wireless charger holder disengagement	<input type="checkbox"/>
15.	Quick-connect actuators connected to UniO system	<input type="checkbox"/>
16.	Check quick-connect actuators action	<input type="checkbox"/>
17.	Semaphore connected to UniO system	<input type="checkbox"/>
18.	Check semaphore is working	<input type="checkbox"/>

-
- 19. Load cell under rocket connected to UniO system
 - 20. Check load cell sensor data
 - 21. Connect igniter to UniO system
 - 22. Check igniter continuity

Signature: _____



Ilustria



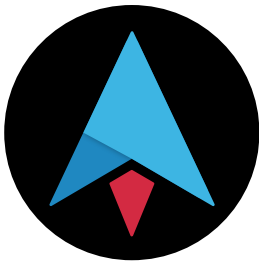
Ignition Checklist

Date: _____

Responsible person: _____

#	Item	Check
1.	Igniter filled	<input type="checkbox"/>
2.	Burners present	<input type="checkbox"/>
3.	Igniter in engine	<input type="checkbox"/>
4.	Cables working	<input type="checkbox"/>
5.	Igniter connected	<input type="checkbox"/>
6.	Software check	<input type="checkbox"/>

Signature: _____



Ilustria



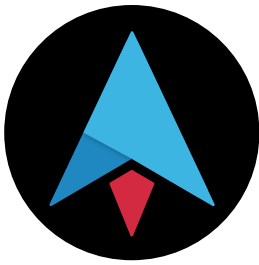
Propulsion Checklist

Date: _____

Responsible person: _____

#	Item	Check
1.	Rocket fluid systems ready	<input type="checkbox"/>
2.	Injector installed	<input type="checkbox"/>
3.	Fuel grain ready	<input type="checkbox"/>
4.	Igniter ready	<input type="checkbox"/>
5.	Spacers ready	<input type="checkbox"/>
6.	Injector head O rings present	<input type="checkbox"/>
7.	Ignition spacer O ring present	<input type="checkbox"/>
8.	Nozzle O rings present	<input type="checkbox"/>
9.	Engine charge assembled	<input type="checkbox"/>
10.	Engine assembled	<input type="checkbox"/>
11.	Injector pressure sensor connected	<input type="checkbox"/>
12.	Chamber pressure sensor connected	<input type="checkbox"/>
13.	Engine secured	<input type="checkbox"/>

Signature: _____



Ilustria



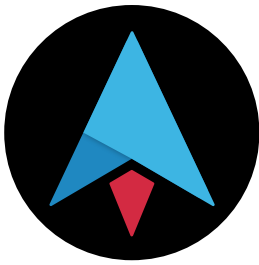
Rocket Fluid Systems Checklist

Date: _____

Responsible person: _____

#	Item	Check
1.	Fluid system assembled	<input type="checkbox"/>
2.	Reduction valve set	<input type="checkbox"/>
3.	Servos connected	<input type="checkbox"/>
4.	Servos operating	<input type="checkbox"/>
5.	Pressure section release valve set	<input type="checkbox"/>
6.	Oxidizer section release valve set	<input type="checkbox"/>
7.	Pressure section pressure sensor set	<input type="checkbox"/>
8.	Oxidizer section pressure sensor set	<input type="checkbox"/>
9.	Oxidizer section temperature sensor set	<input type="checkbox"/>

Signature: _____



Ilustria



GO/NO GO Poll Checklist

Date: _____

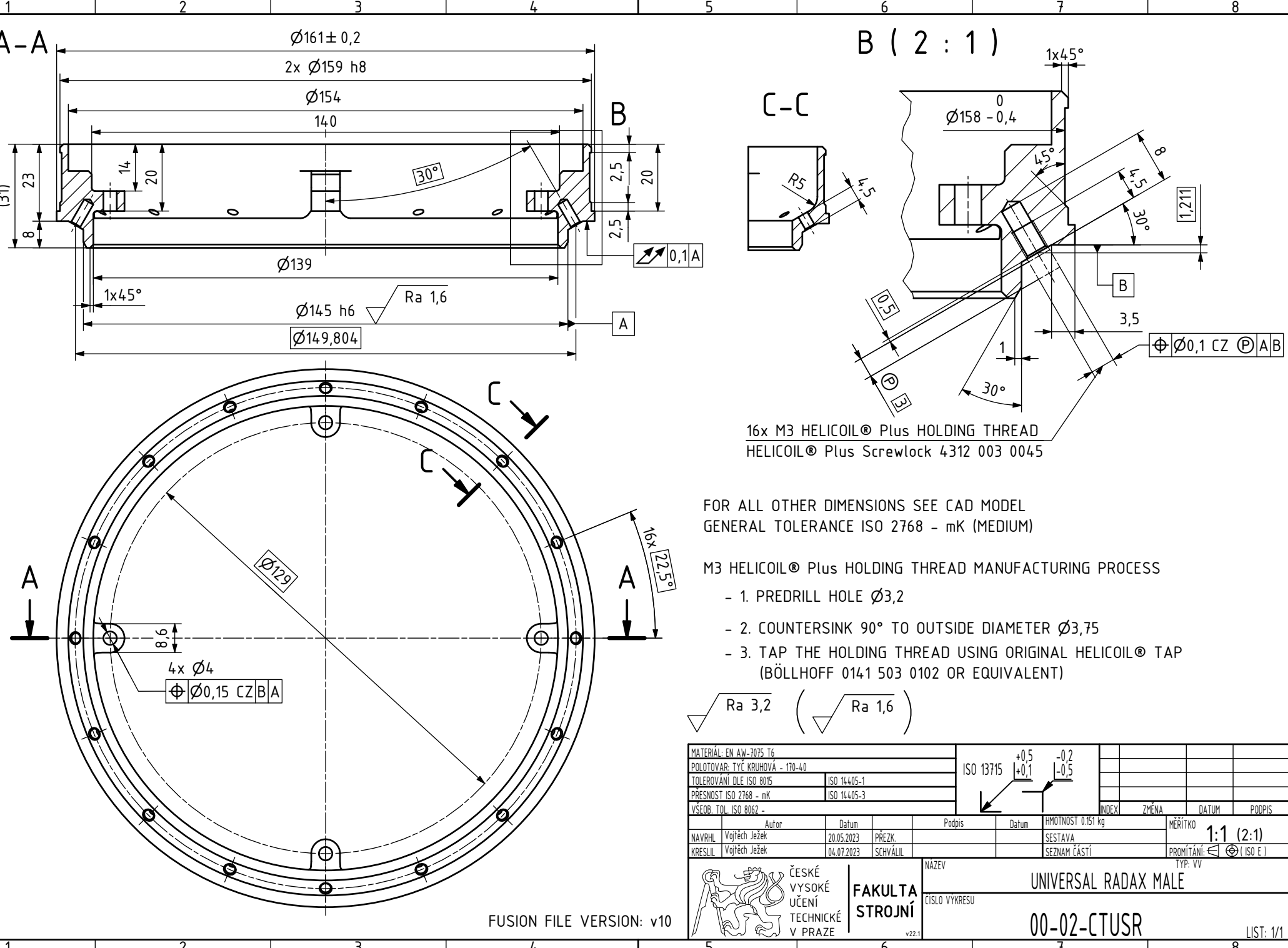
Responsible person: _____

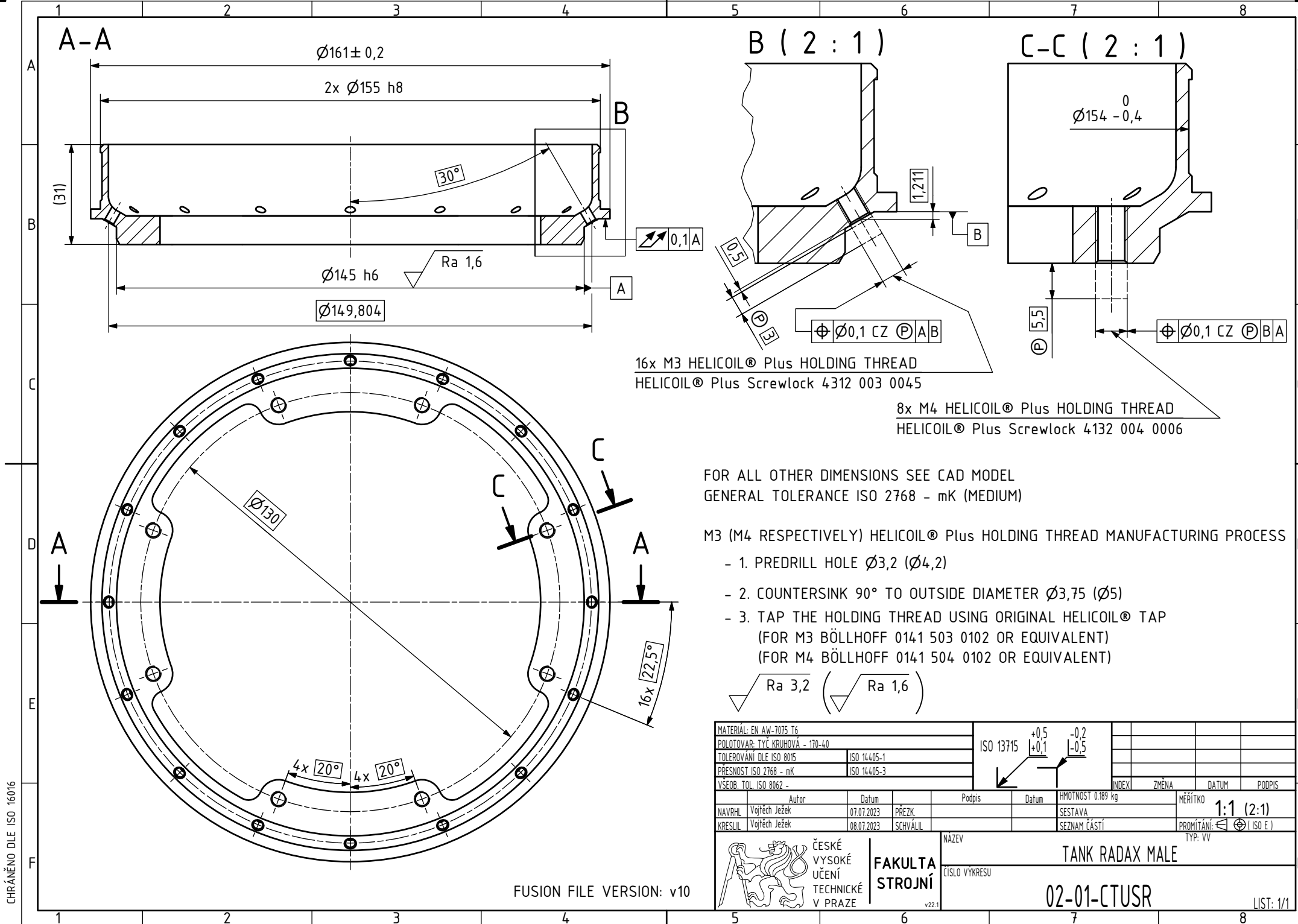
#	Item	Check
1.	Power	<input type="checkbox"/>
2.	Controls	<input type="checkbox"/>
3.	Telemetry	<input type="checkbox"/>
4.	Flight software	<input type="checkbox"/>
5.	COMS	<input type="checkbox"/>
6.	Structure	<input type="checkbox"/>
7.	GSE	<input type="checkbox"/>
8.	Recovery	<input type="checkbox"/>
9.	Ignition	<input type="checkbox"/>
10.	PROP	<input type="checkbox"/>
11.	Range	<input type="checkbox"/>

Signature: _____

5.6 Engineering Drawings

THIS PAGE IS INTENTIONALLY LEFT BLANK





1 2 3 4 5 6 7 8

A

B

C

D

F

1

A →

G 3/8-19

3x G 1/4-19

A →

This diagram shows an exploded view of a bearing assembly. It includes two large outer rings, one inner ring, and several rolling elements (balls or rollers) arranged in a single row.

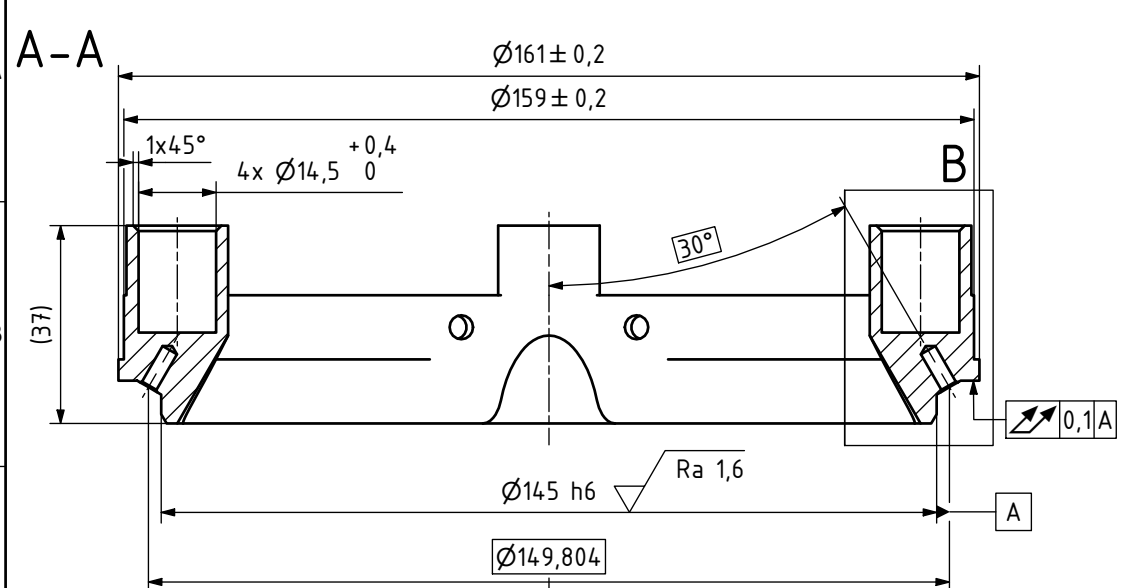
A-A

FOR ALL OTHER DIMENSIONS SEE CAD MODEL
GENERAL TOLERANCE ISO 2768 - mK (MEDIUM)

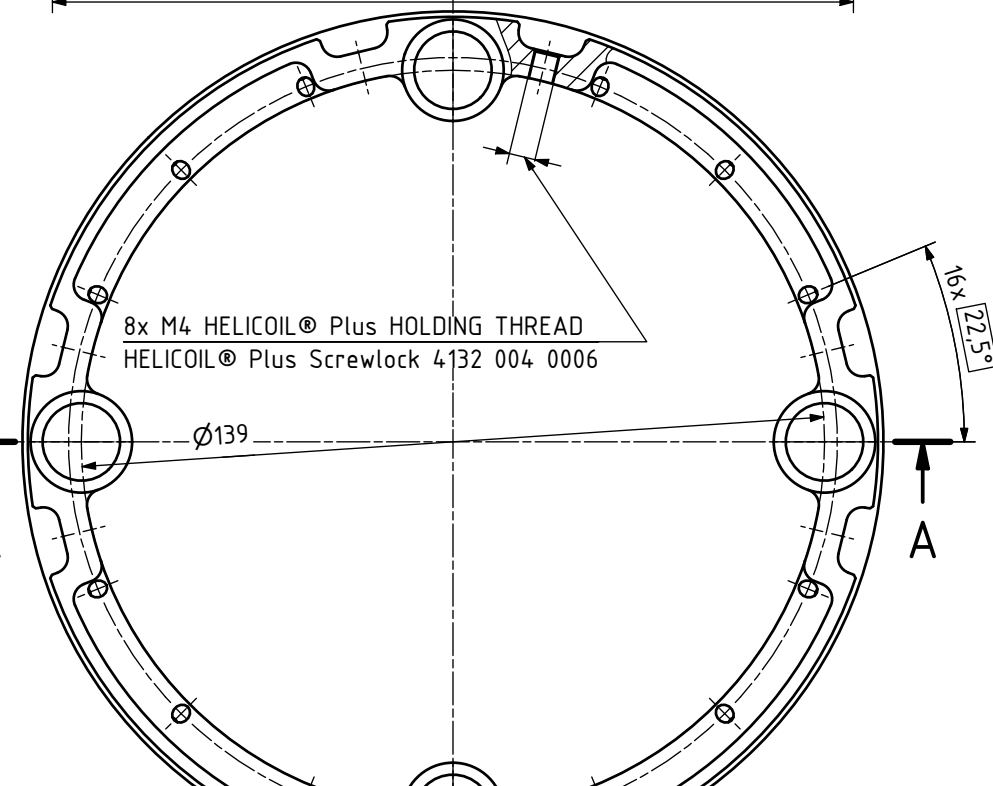
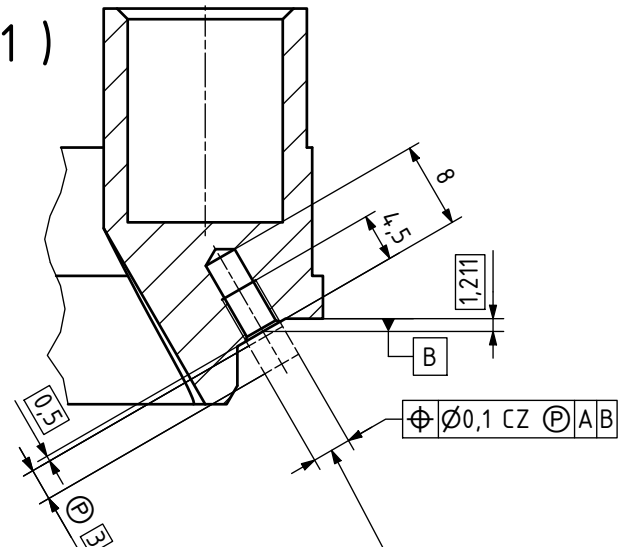
Ra 3,2

MATERIÁL: EN AW-7075 T6							
POLOTOVAR: -		ISO 13715		+0,5 +0,1	-0,2 -0,5		
TOLEROVÁNÍ DLE ISO 8015	ISO 14405-1						
PŘESNOST ISO 2760 - mK	ISO 14405-3						
VSEOB. TOL. ISO 8062 -						INDEX	ZMĚNA
						DATUM	PODPIS
NAVRHL	Autor	Datum	Podpis	Datum	HJMOTNOST 0,519 kg	MĚŘITKO	1:1 (1:2)
Vojtěch Ježek		08.08.2023	PŘEZK.		SESTAVA		
KRESLIL	Vojtěch Ježek	09.08.2023	SCHVÁLIL		SEZNAM ČÁSTÍ	PROMÍTÁNÍ:	(ISO E)
						TYP: VV	
 ČESKÉ VYSOKÉ UČENÍ TECHNICKÉ V PRAZE		FAKULTA STROJNÍ <small>v22.1</small>		NAZEV CÍSLO VYKRESU		NEW TANK CAP 02-04-CTUSR	
						<small>F</small> <small>LIST: 1/1</small>	

FUSION FILE VERSION: v3



B (2 : 1)



FOR ALL OTHER DIMENSIONS SEE CAD MODEL
GENERAL TOLERANCE ISO 2768 - mK (MEDIUM)

M3 (M4 RESPECTIVELY) HELICOIL® Plus HOLDING THREAD MANUFACTURING PROCESS

- 1. PREDRILL HOLE Ø3,2 (Ø4,2)
- 2. COUNTERSINK 90° TO OUTSIDE DIAMETER Ø3,75 (Ø5)
- 3. TAP THE HOLDING THREAD USING ORIGINAL HELICOIL® TAP
(FOR M3 BÖLLHOFF 0141 503 0102 OR EQUIVALENT)
(FOR M4 BÖLLHOFF 0141 504 0102 OR EQUIVALENT)

$\sqrt{Ra\ 3,2}$ ($\sqrt{Ra\ 1,6}$)

MATERIÁL: EN AW-7075 T6	ISO 13715	+0,5	-0,2		INDEX	ZMĚNA	DATUM	PODPIS
POLOTOVÁR: TYČ KRUHOVÁ - 170-45		+0,1	-0,5					
TOLEROVÁNÍ DLE ISO 8015	ISO 14405-1							
PŘESNOST ISO 2768 - mK	ISO 14405-3							
VŠEOB. TOL ISO 8062 -								
NAVRLH: Klára Čepová	Autor:	Datum:	Podpis:	Datum:	HOMOTNOST 0,204 kg	MĚŘITKO	1:1 (2:1)	
KRESLIL: Vojtěch Ježek		03.07.2023		PŘEZK.		SESTAVA		
		06.07.2023	SCHVALIL:			SEZNAM ČÁSTÍ		PROMÍTÁNÍ: (ISO E)



FAKULTA
STROJNÍ

NÁZEV
CÍLOVÝ VÝKRESU
v22.1

PRESSURE RADAX MALE

03-01-CTUSR

LIST: 1/1

1

2

3

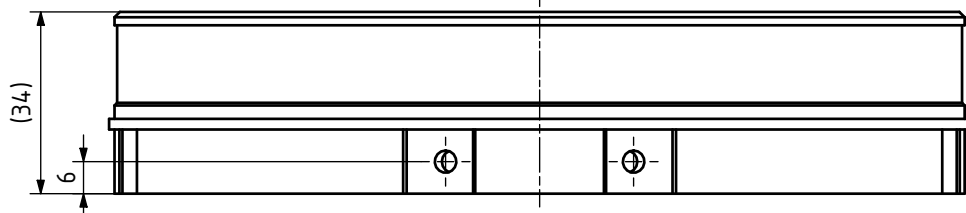
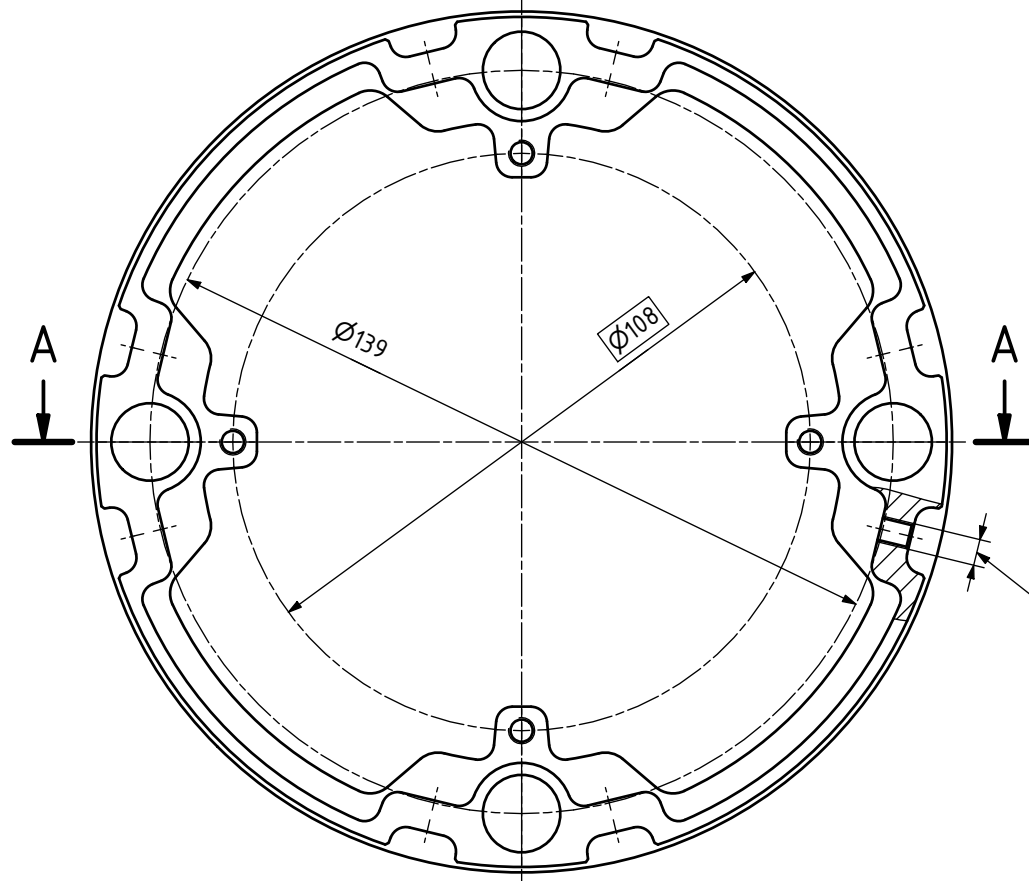
4

5

6

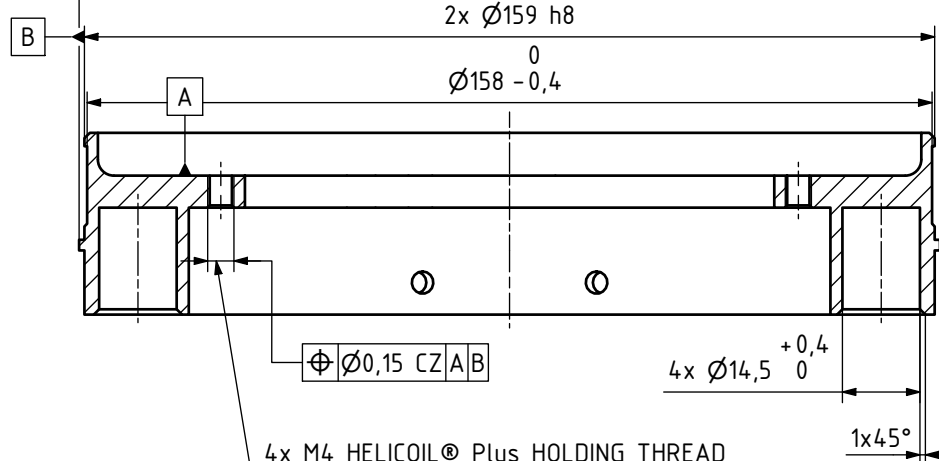
7

8



FUSION FILE VERSION: v20

A-A

 $\varnothing 161 \pm 0,2$ 2x $\varnothing 159$ h80
 $\varnothing 158 -0,4$ 

FOR ALL OTHER DIMENSIONS SEE CAD MODEL
GENERAL TOLERANCE ISO 2768 - mK (MEDIUM)

M4 HELICOIL® Plus HOLDING THREAD MANUFACTURING PROCESS

- 1. PREDRILL HOLE $\varnothing 4,2$
- 2. COUNTERSINK 90° TO OUTSIDE DIAMETER $\varnothing 5$
- 3. TAP THE HOLDING THREAD USING ORIGINAL HELICOIL® TAP (BÖLLHOFF 0141 504 0102 OR EQUIVALENT)

Ra 3,2

MATERIÁL: EN AW-7075 T6	ISO 13715	+0,5	-0,2	INDEX	ZMĚNA	DATUM	PODPIŠ
POLOTOVAR: TYČ KRUHOVÁ - 170-40		+0,1	-0,5				
TOLEROVÁNÍ DLE ISO 8015	ISO 14405-1						
PŘESNOST ISO 2768 - mK	ISO 14405-3						
VŠEOB. TOL ISO 8062 -							
NAVRLH: Klára Čepová	Autor:	Datum:	Podpis:	Datum:	Hmotnost 0,266 kg	MĚŘITKO	1:1
KRESLIL: Vojtěch Ježek		03.07.2023		PŘEZK.	SESTAVA		
		06.07.2023	SCHVALIL:		SEZNAM ČÁSTÍ		
					PROMÍTÁNÍ: (ISO E)		
					NÁZEV		
					K-CONNECTOR		
					CÍLOVÝ KRESLIL		
					03-02-CTUSR		
						LIST: 1/1	



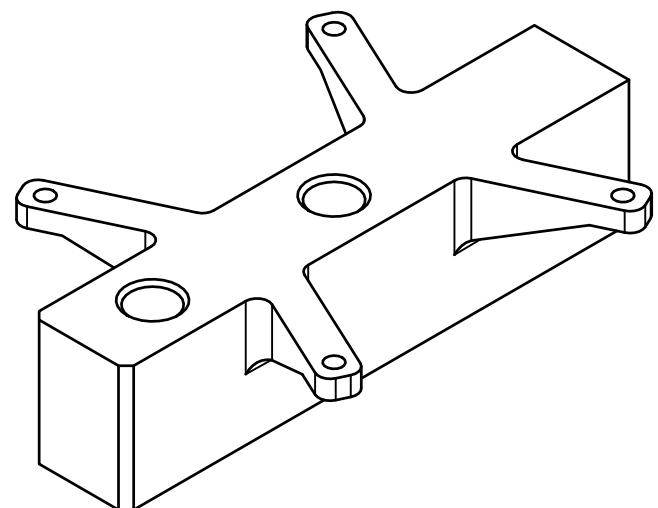
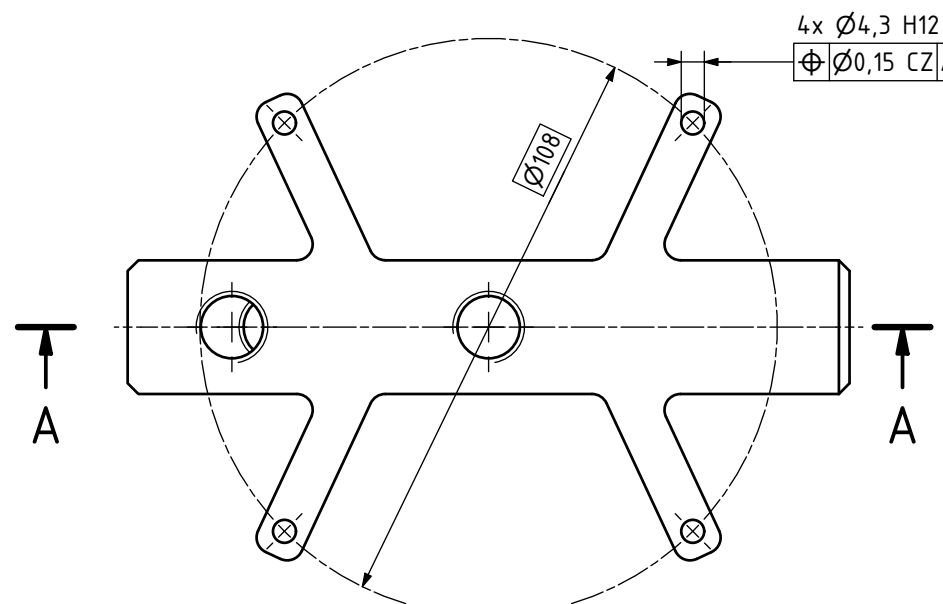
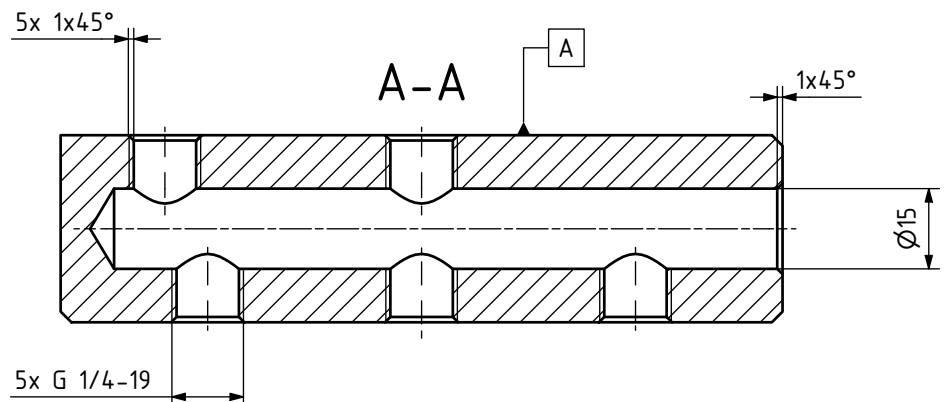
FAKULTA
STROJNÍ

v22.1

NÁZEV
CÍLOVÝ KRESLIL

1 2 3 4 5 6 7 8

A



FOR ALL OTHER DIMENSIONS SEE CAD MODEL
GENERAL TOLERANCE ISO 2768 - mK (MEDIUM)

Ra 3,2

MATERIÁL: EN AW-7075 T6							
POLOTOVAR: -							
TOLEROVÁNÍ DLE ISO 8015		ISO 14405-1		ISO 13715		+0,5 +0,1	-0,2 -0,5
PŘESNOST ISO 2768 - mK		ISO 14405-3					
VŠEOB. TOL. ISO 8062 -						INDEX	ZMĚNA
						DATUM	PODPIS
		Autor	Datum	Podpis		Datum	HOMOTNOST 0,279 kg
NAVHRHL		Hořejší, Čepová	03.08.2023	PRÉZK.			MĚŘITKO
KRESLIL		Vojtěch Ježek	09.08.2023	SCHVALIL			1:1
						SESTAVA	PROMÍTÁNÍ:
						SEZNAM ČÁSTÍ	(ISO E)
						TYP: VV	
 ČESKÉ VYSOKÉ UČENÍ TECHNICKÉ V PRAZE		FAKULTA STROJNÍ	NAZEV		DISTRIBUTION BLOCK		
			ČÍSLO VYKRESU		03-03-CTUSR		
		v22.1			LIST: 1/1		

CHRÁNĚNO DLE ISO 16016

FUSION FILE VERSION: v6

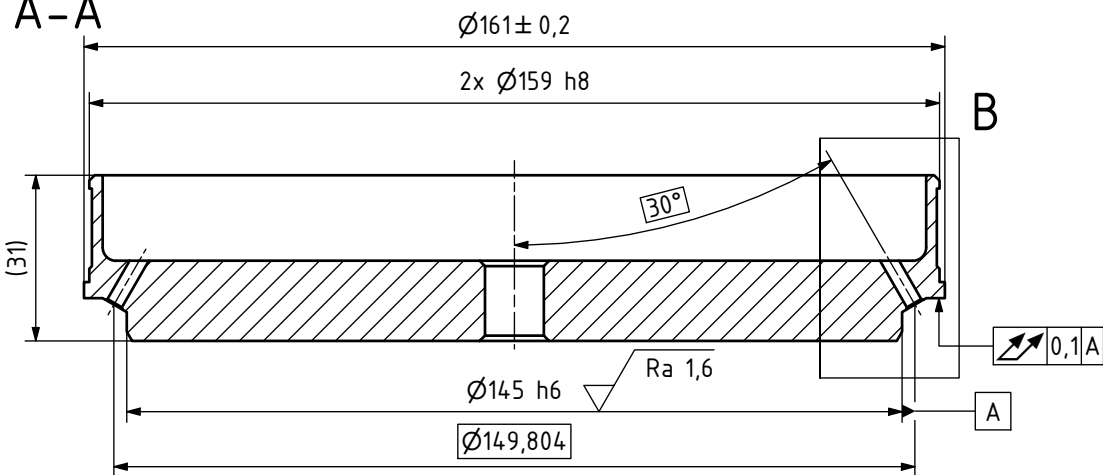
ČESKÉ
VYSOK
UČENÍ
TECHNI
V. PRA
V

NAZEV
FAKULTA
STROJNÍ
CÍLOVÝ KRESL
E

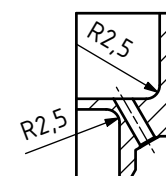
03-03-CTUSR

LIST: 1/1

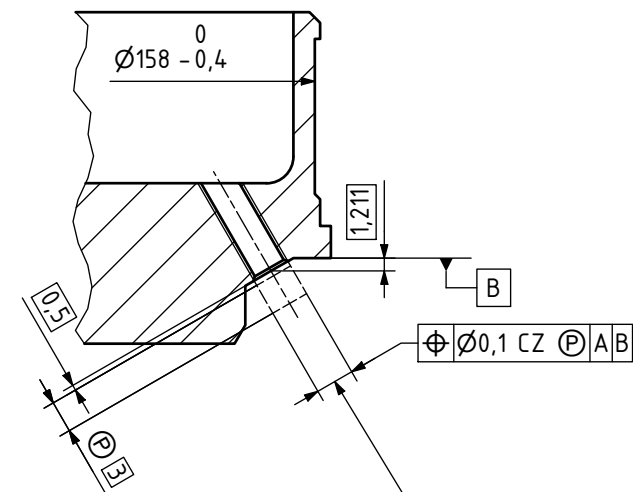
A-A



C-C



B (2 : 1)



FOR ALL OTHER DIMENSIONS SEE CAD MODEL
GENERAL TOLERANCE ISO 2768 - mK (MEDIUM)

M3 HELICOIL® Plus HOLDING THREAD MANUFACTURING PROCESS

- 1. PREDRILL HOLE Ø3,2
- 2. COUNTERSINK 90° TO OUTSIDE DIAMETER Ø3,75
- 3. TAP THE HOLDING THREAD USING ORIGINAL HELICOIL® TAP (BÖLLHOFF 0141 503 0102 OR EQUIVALENT)

$Ra 3,2$ ($Ra 1,6$)

MATERIÁL: EN AW-7075 T6	POLOTOVAR: TYČ KRUHOVÁ - 170-40	ISO 13715	+0,5	-0,2	INDEX	ZMĚNA	DATUM	PODPLIS
POLOTOVAR: TYČ KRUHOVÁ - 170-40	TOLEROVÁNÍ DLE ISO 8015	ISO 14405-1	+0,1	-0,5				
	PŘESNOST ISO 2768 - mK	ISO 14405-3						
VÝROB. TOL ISO 8062 -								
NAVHL: Jakub Hajný	Autor	Datum	Podpis	Datum	HOMOTNOST 0,336 kg	MĚŘITKO	1:1 (2:1)	
KRESLIL: Vojtěch Ježek		03.07.2023		PŘEZK.		SESTAVA		
		07.07.2023	SCHVALIL			SEZNAM ČÁSTÍ		
							PROMÍTÁNÍ: <input checked="" type="checkbox"/> (ISO E)	



FAKULTA
STROJNÍ

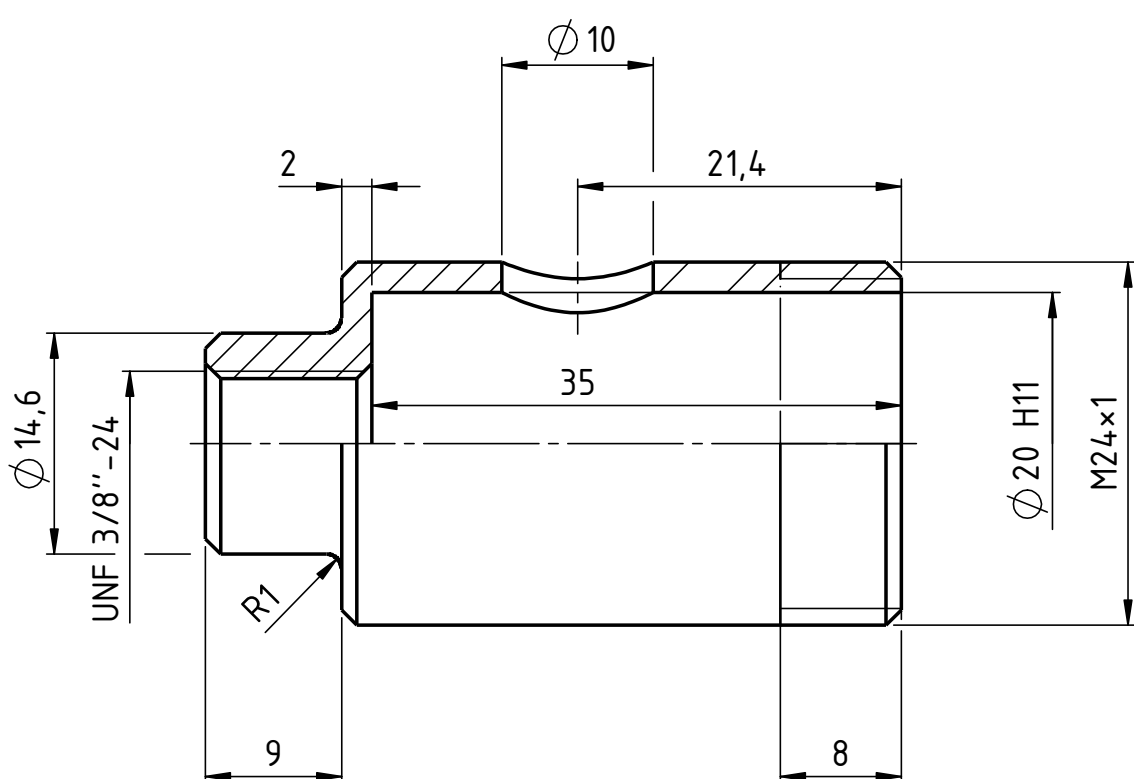
v22.1

NÁZEV
CÍLOVÝ VÝKRESU

RECOVERY RADAX MALE

06-01-CTUSR

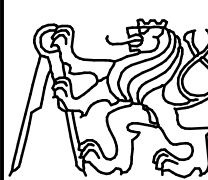
LIST: 1/1



ZKOSENÍ 1x45°

Ra 6,3

MATERIÁL: POLOTOVAR: KR25x50 TOLEROVÁNÍ DLE ISO 8015 PŘESNOST ISO 2768 - mK VŠEOB. TOL. ISO 8062 -			ISO 13715	+0,5 +0,1	-0,2 -0,5				
	Autor	Datum		Podpis	Datum	HMOTNOST -	INDEX	ZMĚNA	DATUM
NAVRHL	HAJNÝ JAKUB	7.2.2023	PŘEZK.			SESTAVA 01-01-06-01-TD		MĚRÍTKO	2:1
KRESL II	HAJNÝ JAKUB	7.2.2023	SCHVÁL II			KUPOVÁNÍ 01-01-06-01K-TD		PROMÍTÁNÍ	(ISO E)



ČESKÉ VYSOKÉ UČENÍ TECHNICKÉ V PRAZE

FAKULTA
STROJNÍ

v21.1

NÁZEV

PYRO VALVE BODY

CÍSLO VÝKRESU

01-01-06-01-01-TD

LIST: 1/1

1

2

3

4

A

B

C

D

E

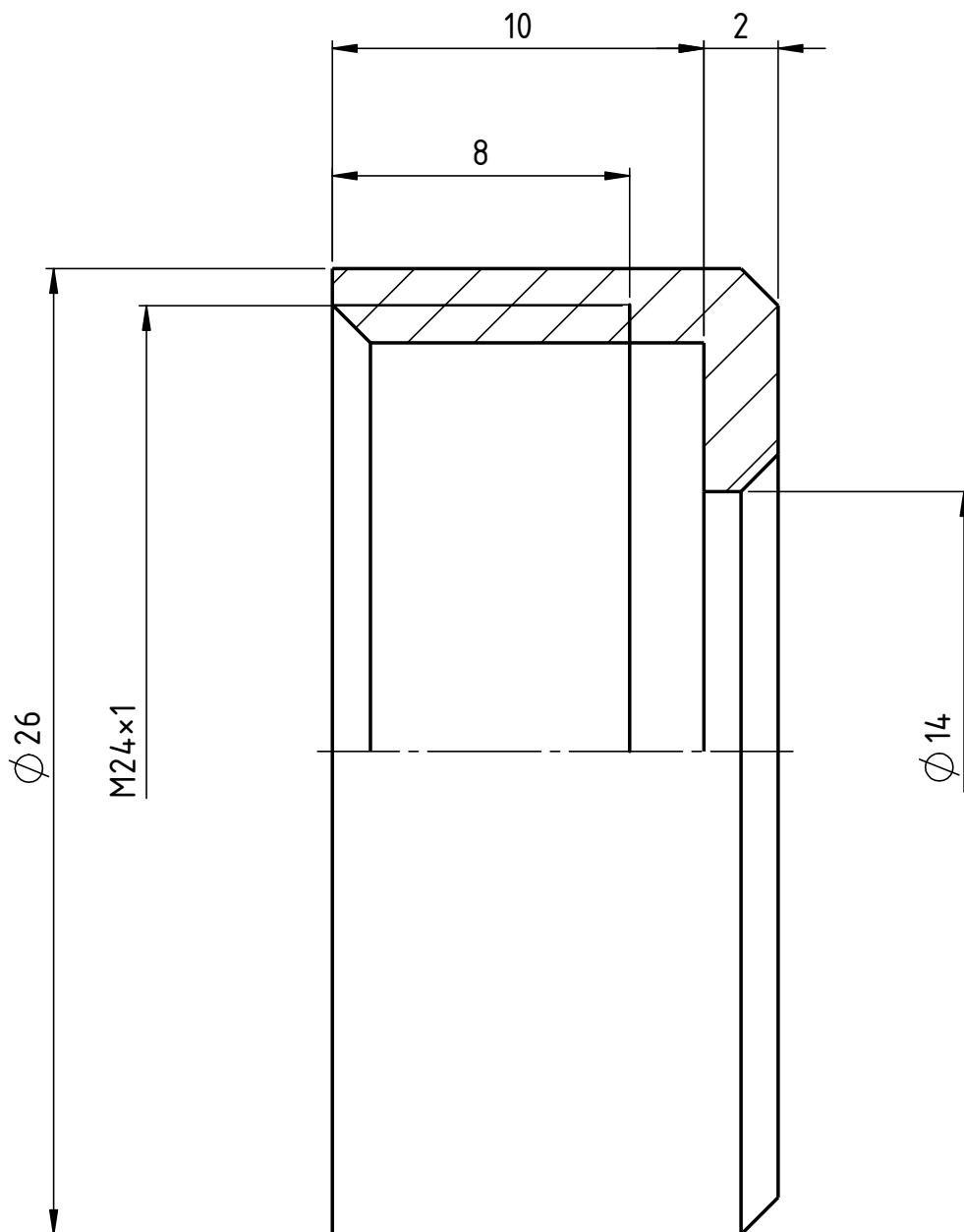
A

B

C

D

E



ZKOSENÍ 1x45°

Ra 6,3

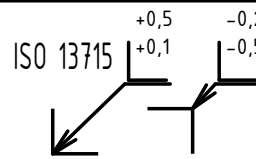
MATERIÁL:

POLOTOVAR: KR27x15

TOLEROVÁNÍ DLE ISO 8015 ISO 14405-1

PŘESNOST ISO 2768 - mK ISO 14405-3

VŠEOB. TOL. ISO 8062 -



INDEX ZMĚNA DATUM PODPIS

	Autor	Datum		Podpis	Datum	HMOTNOST	MĚRÍTKO
NAVRLH	HAJNÝ JAKUB	7.6.2023	PŘZK.			SESTAVA 01-01-06-01-TD	5:1
KRESLIL	HAJNÝ JAKUB	7.6.2023	SCHVÁLIL			KUSOVNÍK 01-01-06-01K-TD	PROMÍTÁNÍ: <input checked="" type="checkbox"/> (ISO E)



ČESKÉ
VYSOKÉ
UČENÍ
TECHNICKÉ
V PRAZE

FAKULTA
STROJNÍ

v211

NÁZEV

PYRO VALVE CAP

ČÍSLO VÝKRESU

01-01-06-01-02-TD

LIST: 1/1

1

2

3

4

5.7 Detailed Logical Process Diagrams

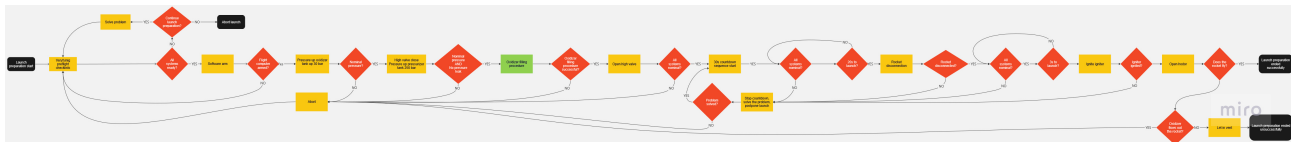


Figure 5.1: ConOps Logic Diagram

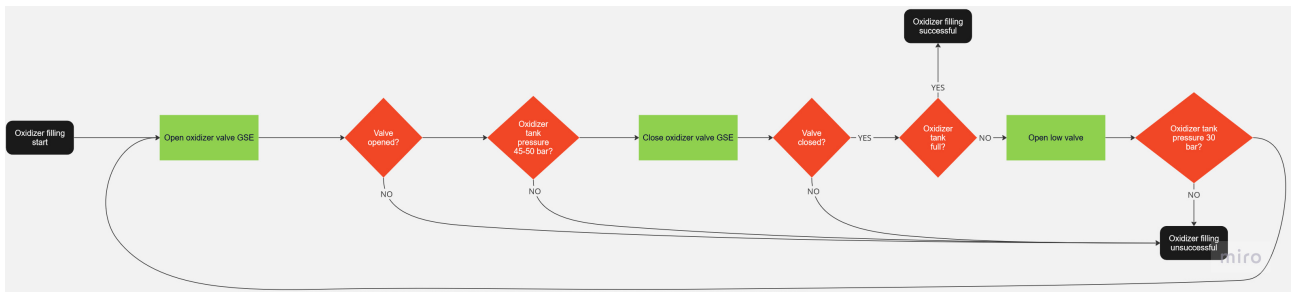


Figure 5.2: Oxidiser Filling Logic Diagram